PHYSICS OF FLUIDS **25**, 125102 (2013)

Partially integrated transport modeling method for turbulence simulation with variable filters

Bruno Chaouat[1,a)] and Roland Schiestel[2]
[1]*ONERA, 92322 Châtillon, France*
[2]*IRPHE, Château-Gombert, 13384 Marseille, France*

(Received 12 July 2013; accepted 11 November 2013; published online 4 December 2013)

The basis of the partially integrated transport modeling method was introduced in papers of Schiestel and Dejoan ["Towards a new partially integrated transport model for coarse grid and unsteady turbulent flow simulations," Theor. Comput. Fluid Dyn. **18**, 443 (2005)] and Chaouat and Schiestel ["A new partially integrated transport model for subgrid-scale stresses and dissipation rate for turbulent developing flows," Phys. Fluids **17**, 065106 (2005)]. This method provides a continuous approach for hybrid Reynolds averaged Navier-Stokes (RANS)-large eddy simulation (LES) simulations with seamless coupling between RANS and LES regions. The method, like in usual LES techniques, makes use of space filtering in the turbulent field. In the foundation papers cited above and in the main applications considered so far, the filter width has been supposed constant or at least slowly varying. In the present paper, we examine the effect of variable filter width in the model equations and how to account for this effect in practical numerical simulations. With the aim to illustrate the theoretical development of the effect of varying filter width in time and space on the governing equations of mass, momentum, and turbulence model, and to show the usefulness of the proposed approach, we perform then numerical simulations of isotropic decaying turbulence. © *2013 AIP Publishing LLC*. [http://dx.doi.org/10.1063/1.4833235]

I. INTRODUCTION

Large eddy simulation[1] (LES) which consists in filtering the instantaneous Navier-Stokes equations with the aim to compute the large scale motions of the flow while the smaller scales are modeled has been developed actively in the past two-decade thanks to the increase of super computer-power[2] and rapidly became a widespread practice. The scale separation is usually made from a filtering operation. But, compared to the statistical averaging used in Reynolds averaged Navier-Stokes (RANS) techniques which satisfies the general Reynolds rules, the filtering operation proved to be more tricky because of non-commutativity with respect to other mathematical operations like products or derivatives. The problem is more acute when using strongly variable mesh steps. In this framework, numerous works and an important literature have been devoted to the study of commutation terms arising from the non-commutativity of the filtering process with temporal or spatial derivatives. More precisely, using a variable filter width will bring new additional terms in the filtered momentum and the turbulence equations because the filtering operation and the derivative operation do not commute exactly. This is generally known as the commutation errors and has given rise to numerous fundamental studies.

Up to now, the LES method, however, is not always affordable for industrial applications involving high Reynolds numbers because of the prohibitive computational time and memory requirements, contrarily to the RANS method which is still often used in industry in practice.[3,4] However, the RANS approach, due to its lack of universality, may lead to difficulties in complex flows. This is the reason which has led researchers involved in the community of turbulence to develop hybrid

a)Electronic mail: Bruno.Chaouat@onera.fr

RANS-LES methods, especially for simulating engineering or industrial flows with acceptable computational resources while retaining some beneficial aspects of the LES approach.[5] Among these hybrid RANS-LES methods, we focus interest in the partially integrated transport modeling (PITM) method introduced by Schiestel and Dejoan[6] using a two equation subfilter scale closure model and by Chaouat and Schiestel[7] for the extension to stress transport subfilter scale models which proved to be a promising route of investigation. This method provides a continuous approach for hybrid RANS-LES simulations with seamless coupling between RANS and LES regions.

Like in usual LES techniques, the PITM method makes use of space filtering in the turbulent field. In the foundation papers cited above and in the main applications considered so far, the filter width has been supposed constant or at least slowly varying in time and in space. But, depending on the type of applications under consideration and the particular geometry of the flow, it may be sometimes necessary to introduce strongly varying meshes and filters of different sizes. The consequence of such a practice is that when the filter width is changed, the amount of resolved turbulence energy relatively to the modeled turbulence energy gets modified.

At the present time, substantial progress has been made on the problem of commutation errors. But many questions still remain open and the development of some practical techniques is desirable in default of a fundamental revision of the approach (involving perhaps some kind of conditional averaging?). A comprehensive overview of the main aspects of the general problem of commutation errors can be found in particular in Ref. 8. The work of Ghosal and Moin[9] was among the first one to properly define and analyze variable filtering in complex geometries. These authors have used a mapping technique from the computational space to a transformed domain with uniform grid in order to derive the commutation error. Then, they were led to define filters that commute up to an error which is of second order in the filter width. Van Der Ven[10] has constructed a family of filters with nonuniform filter widths that commute with differentiation up to any given order. Other authors, such as Fureby and Tabor[11] have examined the different mathematical constraints on the filtering operation in LES and have considered, among all these problems, the commutation error in the filtered Navier-Stokes equations. These authors have shown using a Taylor series expansion that it is possible to get a general expression for the commutation error. Then, they quantified this effect in the fully developed channel flow performed on a non-uniform computational grid. Note that a class of filters for LES calculations of turbulent inhomogeneous flows was presented by Vasilyev *et al.*,[12] giving a general set of rules for constructing discrete filters in complex geometries. With these filters, the commutation error between numerical differentiation and filtering can be made arbitrarily small. A method for constructing discrete filters was also given by Marsden *et al.*,[13] for LES of turbulent flows on unstructured meshes, for which the commutation error between differentiation and filtering can also be made arbitrarily small. As pointed out by Ghosal and Moin[9] and Van Der Ven,[10] it is even possible to derive variable filters that can commute with the derivative, up to a certain fixed order. The authors Iovieno and Tordella[14] gave an interesting new procedure for approximating the noncommutation terms in variable filtering. These approximations make use of an additional super filter $\widetilde{\Delta}$ built with twice the width Δ of the calculation filter in order to evaluate the derivatives $\partial/\partial\Delta$ with respect to Δ. A refined spectral analysis was proposed by Vasilyev and Goldstein[15] to get information about the local spectral content of the commutation error in LES, its dependence on the filter shape and the non-uniformity of the filter width. They illustrated the analysis by performing simulations on homogeneous turbulence. More recently, Hamba[16] evaluated the magnitude of commutation errors by means of LES comparisons with a direct numerical simulation (DNS) of the fully turbulent channel flow. He showed that the noncommutation terms may reach important values and cannot be neglected when performing hybrid RANS-LES simulations. Another harsh aspect of the commutation problem usually appears in zonal hybrid methods at the RANS-LES interface. Most often, the problem arises in wall bounded flows in which the interface is parallel to the wall producing the well known log-layer mismatch.[17] To solve the problem, stochastic forcing[18] is usually introduced in the computational domain as well as also additional filtering.[19] More recently, the work of Hamba[16] emphasized the physical meaning of these commutation terms. As a result of interest, Hamba showed that the commutation terms could be interpreted as additional fluxes in the second moment equations. As expected, this point of view was found in complete agreement with the methods developed very earlier in previous Refs. 20–22. The work of Cubero and Piomelli[23] explored an alternative approach in which the filter width was entirely decoupled from the grid size. The effect of using a variable filter to grid ratio was analyzed in the case of developing channel flow. This method aimed in reducing the numerical errors arising in variable mesh LES. As a result of interest to mention, one can remark that the PITM method relies on subfilter modeling and consequently is directly amenable to such an approach with filtering decoupled with the grid. Even now, the commutation error remains an important issue in LES that is still not solved in a satisfactory way in the literature, and fundamental studies currently developed have led to some major advances. For instance van der Bos and Geurts[25] used *a priori* tests based on DNS data in turbulent mixing layers to validate a new model for the kinetic energy dynamics of the commutator-error. This type of work has been pursued by the same authors using DNS data to get a quantitative comparison between the dynamical importance of the commutator error and the subgrid scale (SGS) stress, as indicated in Ref. 26. In this work, the effect of skewness of the filter on the commutator error was found very important. van der Bos and Geurts[27] also showed that the effect of the commutator errors corresponds to the local source of turbulent flow scales, depending on the variation of the filter width along the flow path. This Lagrangian context suggested significant correlation between the material derivative of the filter width and the production or dissipation of kinetic energy due to the commutator error. This was confirmed by *a priori* analysis in the mixing layer and leaded to a new Lagrangian model. Sudden step refinement in the grid size may produce harsh anomalous effects in the numerical simulation, more evidently unphysical than smooth variations in the grid size. The simulation of a plane channel flow using a block-structured finite volume method made by Fröhlich *et al.*,[24] showed for instance that jumps may happen in the stress profiles at the refinement interface. All these numerical studies were complemented by a more theoretical analysis worked out by Geurts and Holm.[28] It was suggested in particular that rather than controlling the size of the commutator errors by increasing the order of the filter, the commutator error can be more efficiently controlled by the spatial variations in the filter properties. Variable resolution computations in the framework of the PANS (partially averaged Navier-Stokes equations) model initially developed for performing hybrid RANS-LES simulations of turbulent flows have been recently carried on by Girimaji and Wallin.[29] This approach differs somehow from the true commutation error as it deals with spatio-temporal variations of the energy ratios (resolved to modeled ratios). The proposed approach is very practical but inevitably suffers from the use of an empirical Boussinesq closure model for modeling the residual terms, its field of applicability being not known. This technique may be questionable on the physical point of view. Another route to circumvent the problem was to use time filtering like introduced by Pruett.[30] For applications to LES, time filters enjoy some advantages relatively to spatial filters. Among these, they can commute more naturally with differential operators. The properties of the residual stresses have been studied further by Pruett *et al.*[31]

In the present paper, we will examine the effect of variable filter width in the PITM model equations and how to account for this effect in practical numerical simulations. For this method, which is by essence a continuous hybrid RANS-LES method with seamless coupling between the RANS and LES regions, we shall deal with continuous changes in the filter width, so that the noncommutation problem will not be concentrated through an interface but will be in the contrary distributed in the whole field. In a general way, the two possible sources of noncommutation terms included in the equation of the filtered motion appear, on the one hand, in the material derivative and, on the other hand, in the diffusion terms involving the second derivative of the fluid velocity or the first derivative of the stresses. The second contribution, linked to the viscous terms composed by the second derivative in space of the velocity, is more likely to act in low Reynolds number regions. So, the noncommutation terms in the material derivative will be treated here as terms of primary importance. In the PITM method, the subfilter scale stress and dissipation-rate transport equations are coupled to the equations of motion and have to be solved at each time advancement of the computation. Consistency in the treatment of commutation terms for both the momentum equations and the subfilter model is then necessary. Using the rules of convolution operators and a mathematical formalism put in place to handle the filtering process, we will first find the complex expressions of the commutation terms appearing in the filtered Navier-Stoke equations and in the transport equations for the subfilter turbulent energy, the subfilter turbulent stress, and the dissipation-rate. For a purpose of explanation, we will consider the Fourier transform of the dynamic equation of the two-point fluctuating velocity correlation tensor in the wave vector space. We will show that the terms arising from the commutation errors can be indeed related to additional transfer fluxes passing through the cutoff wave number, from the resolved scales to the modeled scales or vice-versa. We will then provide a physical method for evaluating the commutation terms in the physical space using a super filter, in addition to the current filter, as well some possible improvements made in connection with the Kolmogorov law in situation of spectral equilibrium. With the aim to illustrate the theoretical development of the effect of the varying filter width in time and space on the governing equations of mass, momentum, and turbulence model, and to show the usefulness of the proposed approach, we will finally perform numerical simulations of isotropic decaying turbulence on a fixed grid, and on several expanding grids without and with the correction terms arising from the commutation errors.

II. THE AVERAGING PROCESS AND FILTERING APPROACH

A. The averaging process

Turbulent flow of a viscous incompressible fluid is considered. The Reynolds averaged Navier-Stokes method in the statistical approach assumes that the variable $\phi(\boldsymbol{x}, t)$ function varying in time and space can be decomposed into an ensemble average part $\langle\phi\rangle$ and a fluctuating part that embodies all the turbulent scales ϕ' such as $\phi = \langle\phi\rangle + \phi'$. From its definition, the statistical mean is defined as

$$\langle\phi(\boldsymbol{x})\rangle = \lim_{N\to\infty} \frac{1}{N} \sum_{j=1}^{N} \phi_j(\boldsymbol{x}, t), \tag{1}$$

where ϕ_j is the result associated with the j process and N, the total number of realizations of the flow. In practice, if assuming an ergodic assumption, the Reynolds averaging is obtained from time averaging over a sufficiently long period of time T in comparison with the characteristic turbulent time scale given itself by the ratio $\tau = k/\epsilon$ where k and ϵ denote the turbulent energy and its dissipation-rate, respectively. In the case where $T \gg \tau$, one gets

$$\langle\phi(\boldsymbol{x})\rangle = \frac{1}{T} \int_0^T \phi(\boldsymbol{x}, t)\, dt. \tag{2}$$

This approximation cannot be used in unsteady turbulent flows in the mean, except in the particular case of periodic flows in which phase averaging can be used. In most theoretical studies, the mean value is given by statistical averaging which allows a more consistent and general formalism in the turbulence equations.

B. The filtering approach

On the other hand, in large eddy simulations, the variable ϕ is decomposed into a large scale (or resolved part) $\bar{\phi}$ and a subfilter-scale fluctuating part $\phi^>$ or modeled part such that $\phi = \bar{\phi} + \phi^>$. The filtered variable $\bar{\phi}$ is defined by the filtering operation as the convolution with a filter G in space

$$\overline{\phi} = G * \phi \tag{3}$$

that leads to the computation of a variable convolution integral

$$\bar{\phi}(\boldsymbol{x}, t) = \int_{\mathbb{R}^3} G\left[\boldsymbol{x} - \boldsymbol{\xi}, \Delta(\boldsymbol{x}, t)\right] \phi(\boldsymbol{\xi}, t) d\boldsymbol{\xi}. \tag{4}$$

The instantaneous fluctuation ϕ' appearing in RANS methodology contains in fact the large scale fluctuating part $\phi^<$ and the small scale fluctuating part $\phi^>$ such that $\phi' = \phi^< + \phi^>$. So that the instantaneous variable ϕ can then be rewritten like the sum of a mean statistical part $\langle\phi\rangle$, a large scale fluctuating part $\phi^<$ and a small scale fluctuating part $\phi^>$ as follows $\phi = \langle\phi\rangle + \phi^< + \phi^>$. The most commonly used filters in the physical space are the box and Gaussian filters. Using the definition (4), it is obvious to see that the Fourier transform of the filtered variable $\bar{\phi}$ in homogeneous turbulence is simply

$$\widehat{\bar{\phi}}(\boldsymbol{\kappa}, t) = \hat{G}(\boldsymbol{\kappa}, \boldsymbol{\kappa_c})\, \hat{\phi}(\boldsymbol{\kappa}, t), \tag{5}$$

where $\boldsymbol{\kappa_c}$ is the cutoff wave number. If in the spectral space, the filtering operation is naturally defined by the spectral cutoff wave number, the interpretation in the physical space by inverse Fourier transform however leads in this case to some complexities because of the more intricate form of the filter function as shown in Subsection A 1 of the Appendix. Space filtering defined in Eq. (4) is used in most current LES methods, but it is also possible to derive time filtering as introduced in Ref. 31.

III. FILTERED EQUATIONS

A. The effect of varying filter width in time and space

1. Commutation terms

Variable filters in space or time bring new important complexities in the form of the equations and their treatment because additional terms appear when filtering the equations. The issue we want to address in the present paper is how to obtain the filtered Navier-Stokes equations when applying a variable filter and how to approximate efficiently the new terms that are appearing. Let us consider the general case where the filter width varies in time and space, like in the case encountered for usual applications to non-homogeneous flows, involving the variable filter function $G\,[\boldsymbol{\xi}, \Delta(\boldsymbol{x}, t)]$. Due to the fact that the filtering operation does not commute with the space derivative, a commutation term will consequently appear as shown in Subsection A 2 of the Appendix. The partial derivative in space of the variable ϕ is then computed by means of the convolution operator defined in Eq. (4) as

$$\frac{\partial \bar{\phi}}{\partial x_j}(\boldsymbol{x}, t) = \overline{\frac{\partial \phi}{\partial x_j}}(\boldsymbol{x}, t) + \frac{\partial \Delta}{\partial x_j}\frac{\partial \bar{\phi}}{\partial \Delta}(\boldsymbol{x}, t) \tag{6}$$

showing that, in shorthand notation,

$$\frac{\partial \bar{\phi}}{\partial x_j} = \beta_{x_j}(\phi) + \overline{\frac{\partial \phi}{\partial x_j}}, \tag{7}$$

with

$$\beta_{x_j}(\phi) = \frac{\partial \Delta}{\partial x_j}\left(\frac{\partial G}{\partial \Delta} * \phi\right) = \frac{\partial \Delta}{\partial x_j}\frac{\partial}{\partial \Delta}(G * \phi) = \frac{\partial \Delta}{\partial x_j}\frac{\partial \bar{\phi}}{\partial \Delta}. \tag{8}$$

In the same way, transposing this development in time variable, one can easily find that the partial derivative in time is

$$\frac{\partial \bar{\phi}}{\partial t} = \beta_t(\phi) + \overline{\frac{\partial \phi}{\partial t}}, \tag{9}$$

with

$$\beta_t(\phi) = \frac{\partial \Delta}{\partial t}\left(\frac{\partial G}{\partial \Delta} * \phi\right) = \frac{\partial \Delta}{\partial t}\frac{\partial}{\partial \Delta}(G * \phi) = \frac{\partial \Delta}{\partial t}\frac{\partial \bar{\phi}}{\partial \Delta}. \tag{10}$$

With the aim to alleviate the presentation, we will consider first the restrictive case where the convection velocity U_j is assumed to be not fluctuating. Then, the previous formula can be extended to the material derivative

$$\frac{d\phi}{dt} = \frac{\partial \phi}{\partial t} + U_j \frac{\partial \phi}{\partial x_j}. \tag{11}$$

By operating the filter, one gets

$$\overline{\frac{d\phi}{dt}} = \overline{\frac{\partial \phi}{\partial t}} + U_j \overline{\frac{\partial \phi}{\partial x_j}}. \tag{12}$$

Using Eqs. (9) and (7), one obtains

$$\frac{d\bar{\phi}}{dt} = \beta_T(\phi) + \overline{\frac{d\phi}{dt}}, \tag{13}$$

where β_T is a new function pertaining to the material derivative and that reads

$$\beta_T(\phi) = \beta_t(\phi) + U_j\beta_{x_j}(\phi) = \frac{d\Delta}{dt}\left(\frac{\partial G}{\partial \Delta} * \phi\right) = \frac{d\Delta}{dt}\frac{\partial\bar{\phi}}{\partial\Delta}. \tag{14}$$

We now consider the general case where the convection velocity is fluctuating in time like in the Navier-Stokes equations. Most of all, if applying Eq. (7) for $\phi = u_i$, where u_i denotes the instantaneous velocity, using Eq. (8) for evaluation β_{x_j}, one has to remark that the divergence of the filtered velocity is not equal to zero, as usually made in large eddy simulations, but satisfies the equation

$$\overline{\frac{\partial u_j}{\partial x_j}} = \frac{\partial \bar{u}_j}{\partial x_j} - \frac{\partial\Delta}{\partial x_j}\frac{\partial \bar{u}_j}{\partial\Delta} = 0. \tag{15}$$

In the remainder of the text, the material derivative pertaining to the instantaneous flow field will be denoted as

$$\frac{d}{dt} = \frac{\partial}{\partial t} + u_j\frac{\partial}{\partial x_j}. \tag{16}$$

Thus, in the case of an incompressible flow considered here, the material derivative of any quantity ϕ can be written in the following form:

$$\frac{d\phi}{dt} = \frac{\partial\phi}{\partial t} + \frac{\partial(u_j\phi)}{\partial x_j}. \tag{17}$$

In order to distinguish clearly the material derivative following the filtered flow from the material derivative following the instantaneous flow, we introduce a different notation

$$\frac{D}{Dt} = \frac{\partial}{\partial t} + \bar{u}_j\frac{\partial}{\partial x_j}. \tag{18}$$

This is implying that the material derivative for any filtered variable $\bar{\phi}$ reads

$$\frac{D\overline{\phi}}{Dt} = \frac{\partial\overline{\phi}}{\partial t} + \bar{u}_j\frac{\partial\overline{\phi}}{\partial x_j}. \tag{19}$$

Applying the filtering operation on Eq. (17) leads to

$$\overline{\frac{d\phi}{dt}} = \overline{\frac{\partial\phi}{\partial t}} + \overline{\frac{\partial\left(u_j\phi\right)}{\partial x_j}}. \tag{20}$$

Then, using Eqs. (7) and (9) yields

$$\overline{\frac{d\phi}{dt}} = \frac{\partial\bar{\phi}}{\partial t} - \beta_t(\phi) + \frac{\partial(\overline{u_j\phi})}{\partial x_j} - \beta_{x_j}(u_j\phi), \tag{21}$$

with the definitions

$$\beta_t(\phi) = \frac{\partial\Delta}{\partial t}\frac{\partial\bar{\phi}}{\partial\Delta} \tag{22}$$

and

$$\beta_{x_j}(u_j\phi) = \frac{\partial\Delta}{\partial x_j}\frac{\partial(\overline{u_j\phi})}{\partial\Delta}. \tag{23}$$

The correlation $\overline{u_j\phi}$ appearing in Eq. (20) can be developed into the form

$$\overline{u_j\phi} = \bar{u}_j\bar{\phi} + [\overline{u_j\phi} - \bar{u}_j\bar{\phi}] = \bar{u}_j\bar{\phi} + \tau(u_j, \phi), \tag{24}$$

where

$$\tau(u_j,\phi)=\overline{u_j\phi}-\bar{u}_j\bar{\phi}, \tag{25}$$

so that Eq. (21) can be rewritten into the following form including the derivative and the subfilter stresses:

$$\overline{\frac{d\phi}{dt}}=\frac{\partial\bar{\phi}}{\partial t}+\frac{\partial(\bar{u}_j\bar{\phi})}{\partial x_j}+\frac{\partial\tau(u_j,\phi)}{\partial x_j}-\beta_t(\phi)-\beta_{x_j}(u_j\phi). \tag{26}$$

The function $\beta_{x_j}(u_j\phi)$ given by Eq. (23) can be also developed in a more explicit form using the decomposition (24) and one can easily find

$$\beta_t(\phi)=\frac{\partial\Delta}{\partial t}\frac{\partial\bar{\phi}}{\partial\Delta}, \tag{27}$$

$$\beta_{x_j}(u_j\phi)=\frac{\partial\Delta}{\partial x_j}\frac{\partial}{\partial\Delta}\left(\bar{u}_j\bar{\phi}+\tau(u_j,\phi)\right), \tag{28}$$

or

$$\beta_{x_j}(u_j\phi)=\bar{u}_j\frac{\partial\Delta}{\partial x_j}\frac{\partial\overline{\phi}}{\partial\Delta}+\bar{\phi}\frac{\partial\Delta}{\partial x_j}\frac{\partial\bar{u}_j}{\partial\Delta}+\frac{\partial\Delta}{\partial x_j}\frac{\partial}{\partial\Delta}\tau(u_j,\phi)=\bar{u}_j\beta_{x_j}(\phi)+\bar{\phi}\frac{\partial\Delta}{\partial x_j}\frac{\partial\bar{u}_j}{\partial\Delta}+\frac{\partial\Delta}{\partial x_j}\frac{\partial}{\partial\Delta}\tau(u_j,\phi). \tag{29}$$

Equation (28) reveals some interesting points which should be emphasized. The first contribution is pertaining to the material derivative *D*/*Dt* whereas the second term involves the subfilter stresses. Then, the final result will be

$$\overline{\frac{d\phi}{dt}}=\frac{\partial\overline{\phi}}{\partial t}+\frac{\partial(\bar{u}_j\overline{\phi})}{\partial x_j}-\beta_t(\phi)-\bar{u}_j\beta_{x_j}(\phi)+\frac{\partial\tau(u_j,\phi)}{\partial x_j}-\frac{\partial\Delta}{\partial x_j}\frac{\partial\tau(u_j,\phi)}{\partial\Delta}-\bar{\phi}\frac{\partial\Delta}{\partial x_j}\frac{\partial\bar{u}_j}{\partial\Delta}. \tag{30}$$

At this step, it is of importance to note these expressions are exact in a mathematical sense without any approximation. Equation (26) will be the main functional operator that will be used as a base throughout the following work. Using Eq. (15), it is of interest to remark also that the first two terms in the RHS of Eq. (30) can be written equivalently as

$$\frac{\partial\overline{\phi}}{\partial t}+\frac{\partial(\overline{u}_j\overline{\phi})}{\partial x_j}=\frac{D\overline{\phi}}{Dt}+\overline{\phi}\frac{\partial\overline{u}_j}{\partial x_j}=\frac{D\overline{\phi}}{Dt}+\overline{\phi}\frac{\partial\Delta}{\partial x_j}\frac{\partial\overline{u}_j}{\partial\Delta} \tag{31}$$

leading to the alternative expression

$$\overline{\frac{d\phi}{dt}}=\left[\frac{D\overline{\phi}}{Dt}+\frac{\partial\tau(u_j,\phi)}{\partial x_j}\right]-\left[\beta_t(\phi)+\overline{u}_j\beta_{x_j}(\phi)\right]-\frac{\partial\Delta}{\partial x_j}\frac{\partial\tau(u_j,\phi)}{\partial\Delta}. \tag{32}$$

In practice, although Eqs. (21)–(23) can be used in numerical simulations, we suggest in the present work to use the simpler form retaining only the material derivative correction terms. Consequently, the practical approximate equation consisting of neglecting the last term appearing in the RHS of Eq. (32) will be

$$\overline{\frac{d\phi}{dt}}\approx\frac{D\overline{\phi}}{Dt}-\left[\beta_t(\phi)+\bar{u}_j\beta_{x_j}(\phi)\right]+\frac{\partial\tau(u_j,\phi)}{\partial x_j}, \tag{33}$$

where

$$\beta_t(\phi)+\bar{u}_j\beta_{x_j}(\phi)=\frac{\partial\Delta}{\partial t}\frac{\partial\bar{\phi}}{\partial\Delta}+\bar{u}_j\frac{\partial\Delta}{\partial x_j}\frac{\partial\bar{\phi}}{\partial\Delta}=\frac{D\Delta}{Dt}\frac{\partial\bar{\phi}}{\partial\Delta}. \tag{34}$$

The previous equations have been derived for a generic filter of any shape characterized by its width Δ. Obviously, any parameter directly linked to the filter width like $\kappa_c=\pi/\Delta$ can be used. Thus, in the particular case of the spectral splitting filter, one prefers to use as well κ_c for the extra commutation term. In this case, Eqs. (22), (23), (27), and (28) still hold formally but they have to be written now as a function of the cutoff wave number κ_c as follows:

$$\beta_t(\phi) = \frac{\partial \kappa_c}{\partial t}\frac{\partial \bar{\phi}}{\partial \kappa_c}, \tag{35}$$

$$\beta_{x_j}(\phi) = \frac{\partial \kappa_c}{\partial x_j}\frac{\partial \bar{\phi}}{\partial \kappa_c}, \tag{36}$$

$$\beta_{x_j}(u_j\phi) = \frac{\partial \kappa_c}{\partial x_j}\frac{\partial}{\partial \kappa_c}\left(\bar{u}_j\bar{\phi} + \tau(u_j,\phi)\right), \tag{37}$$

or

$$\beta_{x_j}(u_j\phi) = \bar{u}_j\beta_{x_j}(\phi) + \frac{\partial \kappa_c}{\partial x_j}\frac{\partial \tau(u_j,\phi)}{\partial \kappa_c} + \bar{\phi}\frac{\partial \kappa_c}{\partial x_j}\frac{\partial \bar{u}_j}{\partial \kappa_c}. \tag{38}$$

In the particular case of a spectral splitting, the commutation term $\beta_t(\phi)$ can be expressed analytically[20] as shown in Subsection A 3 of the Appendix.

2. Consequences on energies

Let us apply Eq. (21) for $\phi = u_i$. One can easily obtain, taking account Eqs. (22) and (23)

$$\overline{\frac{du_i}{dt}} = \frac{\partial \bar{u}_i}{\partial t} + \frac{\partial(\overline{u_i u_j})}{\partial x_j} - \frac{\partial \Delta}{\partial t}\frac{\partial \bar{u}_i}{\partial \Delta} - \frac{\partial \Delta}{\partial x_j}\frac{\partial(\overline{u_i u_j})}{\partial \Delta} \tag{39}$$

or equivalently, if using Eq. (26)

$$\overline{\frac{du_i}{dt}} = \frac{\partial \bar{u}_i}{\partial t} + \frac{\partial(\bar{u}_j\bar{u}_i)}{\partial x_j} + \frac{\partial \tau(u_j,u_i)}{\partial x_j} - \frac{\partial \Delta}{\partial t}\frac{\partial \bar{u}_i}{\partial \Delta} - \frac{\partial \Delta}{\partial x_j}\frac{\partial}{\partial \Delta}\left(\bar{u}_j\bar{u}_i + \tau(u_j,u_i)\right), \tag{40}$$

where

$$\tau(u_i,u_j) = \tau_{ij} = \overline{u_i u_j} - \bar{u}_i\bar{u}_j. \tag{41}$$

In order to get an expression of the material derivative of the kinetic energy, the left and right hand sides of Eq. (40) are multiplied by $\bar{u}_i$ with tensorial contraction. Taking into account Eq. (15), one can easily obtain

$$\begin{aligned}\bar{u}_i\overline{\frac{du_i}{dt}} &= \frac{\partial}{\partial t}\left(\frac{\bar{u}_i\bar{u}_i}{2}\right) + \bar{u}_j\frac{\partial}{\partial x_j}\left(\frac{\bar{u}_i\bar{u}_i}{2}\right) + \bar{u}_i\bar{u}_i\frac{\partial \Delta}{\partial x_j}\frac{\partial \bar{u}_j}{\partial \Delta}\\ &+\bar{u}_i\frac{\partial \tau(u_j,u_i)}{\partial x_j} - \frac{\partial \Delta}{\partial t}\frac{\partial}{\partial \Delta}\left(\frac{\bar{u}_i\bar{u}_i}{2}\right) - \bar{u}_i\frac{\partial \Delta}{\partial x_j}\frac{\partial}{\partial \Delta}\left(\bar{u}_j\bar{u}_i + \tau(u_j,u_i)\right)\end{aligned} \tag{42}$$

and consequently,

$$\frac{D}{Dt}\left(\frac{\bar{u}_i\bar{u}_i}{2}\right) = \bar{u}_i\overline{\frac{du_i}{dt}} + \frac{\partial \Delta}{\partial t}\frac{\partial}{\partial \Delta}\left(\frac{\bar{u}_i\bar{u}_i}{2}\right) + \bar{u}_j\frac{\partial \Delta}{\partial x_j}\frac{\partial}{\partial \Delta}\left(\frac{\bar{u}_i\bar{u}_i}{2}\right) - \bar{u}_i\frac{\partial \tau(u_j,u_i)}{\partial x_j} + \bar{u}_i\frac{\partial \Delta}{\partial x_j}\frac{\partial \tau(u_j,u_i)}{\partial \Delta}. \tag{43}$$

This equation takes on a complex form because of the partial derivatives in space. However, it can be simplified if considering only homogeneous flows in the statistical sense and if we assume also that the filter width Δ varies only in time (according to the homogeneity hypothesis). In this particular case, the statistical averaging of Eq. (42) or (43) leads to

$$\frac{\partial}{\partial t}\left\langle\frac{\bar{u}_i\bar{u}_i}{2}\right\rangle = \left\langle\bar{u}_i\overline{\frac{du_i}{dt}}\right\rangle + \frac{\partial \Delta}{\partial t}\frac{\partial}{\partial \Delta}\left\langle\frac{\bar{u}_i\bar{u}_i}{2}\right\rangle - \left\langle\bar{u}_i\frac{\partial \tau_{ij}}{\partial x_j}\right\rangle. \tag{44}$$

B. Statistical interpretation in the spatial and spectral spaces for the cutoff wave number filter

The best way to understand the effect of the filter is to work directly in the spectral space. In this section, we consider the case of homogeneous anisotropic turbulence with a constant mean velocity gradient to get the more general development as possible. We assume that the cutoff wave number κ_c is only a function of time $\kappa_c = \kappa_c(t)$ for the sake of simplicity. The present reasoning will be developed in the statistical sense. The objective is to see that a part of the commutation term can be indeed interpreted through statistical spectral partitioning. To prove this assertion, we need to refer to the dynamic equation for the two point correlation spectral tensor in one-dimensional spectral space which is the key equation in this framework. The transport equation of the one-dimensional spectral tensor of the double velocity correlations is obtained by taking the Fourier transform and mean integration over spherical shells from the transport equation for the double velocity correlation in physical space. Spherical averages lead to a loss of directional information but the resulting equation gains in simplicity, the averaged spectral correlations being then only function of the wavenumber and no longer of the wavevector.[22,32–35] As a result these equations formally read[22,32,36]

$$\frac{\mathcal{D}\varphi_{ij}(\boldsymbol{X},\kappa)}{\mathcal{D}t} = \mathcal{P}_{ij}(\boldsymbol{X},\kappa) + \mathcal{T}_{ij}(\boldsymbol{X},\kappa) + \Psi_{ij}(\boldsymbol{X},\kappa) + \mathcal{J}_{ij}(\boldsymbol{X},\kappa) - \mathcal{E}_{ij}(\boldsymbol{X},\kappa) \tag{45}$$

and the different terms appearing in the right-hand side of Eq. (45) are, respectively, the production, transfer, redistribution, diffusion, and dissipation contributions. In this equation, the variable $\boldsymbol{X}$ precisely denotes the midway position $\boldsymbol{X} = \frac{1}{2}(\boldsymbol{x}_A + \boldsymbol{x}_B)$ between the two points $\boldsymbol{x}_A$ and $\boldsymbol{x}_B$ introduced as the reference location in space. Equation (45) is written in order to account also for locally homogeneous anisotropic turbulence in which a tangent homogeneous space may vary from one physical point $\boldsymbol{X}$ to another. The mean material derivative is defined as

$$\frac{\mathcal{D}}{\mathcal{D}t} = \frac{\partial}{\partial t} + \langle u_j \rangle \frac{\partial}{\partial X_j} \tag{46}$$

and reduces to $\partial/\partial t$ in the case of strictly homogeneous turbulence. The integration of Eq. (45) over the range $[\kappa_{m-1}, \kappa_m]$ provides the transport equation for the partial turbulent stress $\tau_{ij}^{(m)}$ (Refs. 22 and 36)

$$\frac{\mathcal{D}\tau_{ij}^{(m)}}{\mathcal{D}t} = P_{ij}^{(m)} + \mathcal{F}_{ij}^{(m-1)} + \mathcal{K}_{ij}^{(m-1)} - \mathcal{F}_{ij}^{(m)} - \mathcal{K}_{ij}^{(m)} + \Pi_{ij}^{(m)} + J_{ij}^{(m)} - \epsilon_{ij}^{(m)}, \tag{47}$$

where in this equation, $\mathcal{F}_{ij}^{(m)}$ denotes the cascade transfer, $\mathcal{K}_{ij}^{(m)}$ is the additional flux due to the variation in the spectrum splitting and $\epsilon_{ij}^{(m)}$ is the partial dissipation-rate within the range $[\kappa_{m-1}, \kappa_m]$. These quantities are defined by

$$\tau_{ij}^{(m)} = \int_{\kappa_{m-1}}^{\kappa_m} \varphi_{ij}(\boldsymbol{X},\kappa)d\kappa, \tag{48}$$

$$P_{ij}^{(m)} = -\int_{\kappa_{m-1}}^{\kappa_m} \varphi_{ij}(\boldsymbol{X},\kappa)\frac{\partial \langle u_i \rangle}{\partial x_j}d\kappa, \tag{49}$$

$$\mathcal{F}_{ij}^{(m)} = -\int_{0}^{\kappa_m} \mathcal{T}_{ij}(\boldsymbol{X},\kappa)d\kappa, \tag{50}$$

$$\mathcal{K}_{ij}^{(m)} = -\varphi_{ij}(\boldsymbol{X},\kappa_m)\frac{\partial \kappa_m}{\partial t}, \tag{51}$$

$$\Pi_{ij}^{(m)} = \int_{\kappa_{m-1}}^{\kappa_m} \Psi_{ij}(\boldsymbol{X},\kappa)d\kappa, \tag{52}$$

and

$$\epsilon_{ij}^{(m)} = \int_{\kappa_{m-1}}^{\kappa_m} \mathcal{E}_{ij}(\boldsymbol{X},\kappa)d\kappa. \tag{53}$$

Applying the general equation (47) to the particular range of wave numbers $[0, \kappa_c]$, $[\kappa_c, \kappa_d]$, and $[\kappa_d, \infty[$ yields the exact partially integrated transport equations in a statistical sense that read

$$\frac{\mathcal{D}\tau_{ij}^{(1)}}{\mathcal{D}t} = P_{ij}^{(1)} - \mathcal{F}_{ij}^{(1)} - \mathcal{K}_{ij}^{(1)} + \Pi_{ij}^{(1)} + J_{ij}^{(1)} - \epsilon_{ij}^{(1)}, \tag{54}$$

$$\frac{\mathcal{D}\tau_{ij}^{(2)}}{\mathcal{D}t} = P_{ij}^{(2)} + \mathcal{F}_{ij}^{(1)} + \mathcal{K}_{ij}^{(1)} - \mathcal{F}_{ij}^{(2)} - \mathcal{K}_{ij}^{(2)} + \Pi_{ij}^{(2)} + J_{ij}^{(2)} - \epsilon_{ij}^{(2)}, \tag{55}$$

and

$$\mathcal{F}_{ij}^{(2)} + \mathcal{K}_{ij}^{(2)} = \epsilon_{ij}^{(3)}. \tag{56}$$

As a result of interest, one can see that the term $\mathcal{K}_{ij}^{(1)}$ computed for κ_c using the relation (51)

$$\mathcal{K}_{ij}^{(1)} = -\varphi_{ij}(\boldsymbol{X}, \kappa_c)\frac{\partial \kappa_c}{\partial t}, \tag{57}$$

corresponding to the extra flux due to the variation in the cutoff location can be indeed interpreted as a commutation error. In particular, one can obtain the transport equation for the resolved turbulence energy by tensorial contraction of Eq. (54) leading to

$$\frac{\mathcal{D}k^{(1)}}{\mathcal{D}t} = P^{(1)} - \mathcal{F}^{(1)} + E(\kappa_c)\frac{\partial \kappa_c}{\partial t} + J^{(1)} - \epsilon^{(1)}. \tag{58}$$

Equation (58) allows to determine the role played by the term involving the variation in the cutoff wave number on the resolved scales. Indeed, in the case where the grid size increases with time $\partial\Delta(t)/\partial t > 0$ or $E(\kappa_c)\partial\kappa_c/\partial t < 0$, then a part of the energy contained into the resolved scales is removed and fed into the modeled spectral zone, whereas on the contrary, when $\partial\Delta(t)/\partial t < 0$ or $E(\kappa_c)\partial\kappa_c/\partial t > 0$, a part of energy coming from the modeled zone is injected into the resolved scales . Equation (58) can be formally recovered in strictly homogeneous turbulence (the turbulence diffusion term vanishes in this case) by taking the derivative of the density spectrum itself:

$$\frac{\partial}{\partial t}\int_0^{\kappa_c} E(\kappa, t)d\kappa = \int_0^{\kappa_c} \frac{\partial E(\kappa, t)}{\partial t}d\kappa + E(\kappa_c)\frac{\partial \kappa_c}{\partial t}, \tag{59}$$

with the correspondence of terms

$$\frac{\partial}{\partial t}\int_0^{\kappa_c} E(\kappa, t)d\kappa = \frac{\partial k^{(1)}}{\partial t} \tag{60}$$

and

$$\int_0^{\kappa_c} \frac{\partial E(\kappa, t)}{\partial t}d\kappa = \frac{1}{2}\int_0^{\kappa_c} \left[\mathcal{P}_{jj}(\kappa) + \mathcal{T}_{jj}(\kappa) - \mathcal{E}_{jj}(\kappa)\right]d\kappa = P^{(1)} - \mathcal{F}^{(1)} - \varepsilon^{(1)}. \tag{61}$$

Such extra terms coming from the material derivative are a key feature of the split spectrum models introduced several years ago in Refs. 20–22 and also described in Ref. 37. It is of interest to make the term by term correspondence with Eq. (44) that can be rewritten equivalently (using a time varying cutoff κ_c instead of Δ) as

$$\frac{\partial}{\partial t}\left\langle \frac{\bar{u}_i\bar{u}_i}{2}\right\rangle = \left\langle \bar{u}_i \overline{\frac{du_i}{dt}}\right\rangle + \frac{\partial}{\partial \kappa_c}\left\langle \frac{\bar{u}_i\bar{u}_i}{2}\right\rangle \frac{\partial \kappa_c}{\partial t} - \left\langle \bar{u}_i \frac{\partial \tau_{ij}}{\partial x_j}\right\rangle, \tag{62}$$

showing that $\partial\left\langle \frac{1}{2}\bar{u}_i\bar{u}_j\right\rangle/\partial\kappa_c$ is nothing more than the energy spectrum $E(\kappa_c)$ and especially provides a physical interpretation of the commutation term as also illustrated in Subsection A 4 of the Appendix. All these developments and their physical interpretations are in agreement with the work of Hamba.[16] One remarks also that the first term in the RHS of Eq. (62) is just another equivalent expression of the term appearing in the LHS of Eq. (61).

C. General method to derive filtered equations with varying filters

In this section, we will show how to derive filtered equations with varying filters and analyze what are the approximations that must be reasonably conceded in view to perform a practical numerical simulation without being impeded by cumbersome equations. The basic equations of fluid mechanics and the turbulence constitutive equations usually take the form of transport equations in which the left hand side is the material derivative and the right hand side contains several terms involving more or less complex mathematical products and derivatives of the flow field variables. The material derivative has been already analyzed in Sec. III A 1. Let us consider now several typical situations for the right hand side that may serve as templates for developing the method in general cases.

1. The first derivative

We are considering the first derivative of some quantity ψ and its filtered expression using Eq. (7):

$$\overline{\frac{\partial \psi}{\partial x_j}} = \frac{\partial \bar{\psi}}{\partial x_j} - \frac{\partial \Delta}{\partial x_j}\frac{\partial \bar{\psi}}{\partial \Delta}. \tag{63}$$

2. Higher order derivatives

Considering now

$$\psi = \frac{\partial \chi}{\partial x_k}$$

allows to derive directly the expression for the filtered second derivative $\overline{\partial^2 \chi/\partial x_j \partial x_k}$. Applying two times Eq. (7) gives

$$\overline{\frac{\partial^2 \chi}{\partial x_j \partial x_k}} = \overline{\frac{\partial}{\partial x_j}\left(\frac{\partial \chi}{\partial x_k}\right)} = \frac{\partial}{\partial x_j}\left(\overline{\frac{\partial \chi}{\partial x_k}}\right) - \frac{\partial \Delta}{\partial x_j}\frac{\partial}{\partial \Delta}\left(\overline{\frac{\partial \chi}{\partial x_k}}\right), \tag{64}$$

leading to

$$\overline{\frac{\partial^2 \chi}{\partial x_j \partial x_k}} = \frac{\partial^2 \bar{\chi}}{\partial x_j \partial x_k} - \frac{\partial^2 \Delta}{\partial x_j \partial x_k}\frac{\partial \bar{\chi}}{\partial \Delta} - \frac{\partial \Delta}{\partial x_j}\frac{\partial \Delta}{\partial x_k}\frac{\partial^2 \bar{\chi}}{\partial \Delta \partial \Delta} - \frac{\partial \Delta}{\partial x_k}\frac{\partial^2 \bar{\chi}}{\partial x_j \partial \Delta} - \frac{\partial \Delta}{\partial x_j}\frac{\partial^2 \bar{\chi}}{\partial x_k \partial \Delta}, \tag{65}$$

which is of course a symmetric form with respect to the coordinates x_j and x_k. Dealing with the higher order derivatives can be performed in the same manner, but the equations become even more complex.

3. Product of two variables

The product of two variables such as $(\psi \chi)$ requires the introduction of the correlation of the fluctuations

$$\tau(\psi, \chi) = \overline{\psi \chi} - \overline{\psi}\,\overline{\chi}$$

and then

$$\overline{\frac{\partial \psi \chi}{\partial x_j}} = \frac{\partial \overline{\psi \chi}}{\partial x_j} - \frac{\partial \Delta}{\partial x_j}\frac{\partial \overline{\psi \chi}}{\partial \Delta}$$

and

$$\overline{\frac{\partial \psi \chi}{\partial x_j}} = \frac{\partial \overline{\psi}\,\overline{\chi}}{\partial x_j} - \frac{\partial \Delta}{\partial x_j}\frac{\partial \overline{\psi}\,\overline{\chi}}{\partial \Delta} + \frac{\partial \tau(\psi, \chi)}{\partial x_j} - \frac{\partial \Delta}{\partial x_j}\frac{\partial \tau(\psi, \chi)}{\partial \Delta}.$$

4. Approximations in practical flow simulations

Consider a generic turbulence transport equation of the form as

$$\frac{d\psi}{dt} = f\,(\psi, \mathcal{Z}), \tag{66}$$

in which ψ is some turbulence field variable and $f\,(\psi, \mathcal{Z})$ contains several terms involving more or less complicated mathematical expressions with various multiplications and derivations. The filtered equation is

$$\overline{\frac{d\psi}{dt}} = \overline{f(\psi, \mathcal{Z})}.$$

The filtered material derivative in the LHS can be calculated from Eq. (26) so that

$$\overline{\frac{d\psi}{dt}} = \frac{\partial\bar{\psi}}{\partial t} + \frac{\partial(\bar{u}_j\bar{\psi})}{\partial x_j} + \frac{\partial\tau(u_j,\psi)}{\partial x_j} - \frac{\partial\Delta}{\partial t}\frac{\partial\bar{\psi}}{\partial\Delta} - \frac{\partial\Delta}{\partial x_j}\frac{\overline{(u_j\psi)}}{\partial\Delta} \tag{67}$$

or equivalently if using Eq. (32)

$$\overline{\frac{d\psi}{dt}} = \frac{D\overline{\psi}}{Dt} + \frac{\partial\tau(u_j,\psi)}{\partial x_j} - \frac{D\Delta}{Dt}\frac{\partial\overline{\psi}}{\partial\Delta} - \frac{\partial\Delta}{\partial x_j}\frac{\partial\tau(u_j,\psi)}{\partial\Delta}, \tag{68}$$

$$\frac{D\Delta}{Dt} = \frac{\partial\Delta}{\partial t} + \bar{u}_k\frac{\partial\Delta}{\partial x_k}. \tag{69}$$

Then, the filtered transport Eq. (66) can be written in the general form as

$$\frac{D\overline{\psi}}{Dt} = \overline{f(\psi, Z)} - \frac{\partial\tau(u_j,\psi)}{\partial x_j} + \frac{D\Delta}{Dt}\frac{\partial\overline{\psi}}{\partial\Delta} + \frac{\partial\Delta}{\partial x_j}\frac{\partial\tau(u_j,\psi)}{\partial\Delta}. \tag{70}$$

It is foreseeable that in most cases, the function *f* being ever so little complicated, the resulting Eq. (70) will become nearly intractable. So, to remain as simple as possible for conducting computer applications in real flows, we suggest to retain only the non-commutative term arising from the material derivative and we will discard the other commutation terms coming from the RHS of the model equation (66). The final approximate equation for practical applications then reads

$$\frac{D\overline{\psi}}{Dt} = f(\overline{\psi}, \overline{Z}) - \frac{\partial\tau(u_j,\psi)}{\partial x_j} + \frac{D\Delta}{Dt}\frac{\partial\bar{\psi}}{\partial\Delta}. \tag{71}$$

This approximation corresponds in fact to the relation (12) in which the advection velocity was considered as constant. There is another argument in favor of approximation (71) suggested by the following remark. When considering the statistical mean of turbulence kinetic energy, the second term on the RHS of Eq. (71) is the only term that gives rise to the extra transfer term in Eq. (59). In practice, we shall remind that, it is only necessary to apply Eq. (12) to derive these practical approximations. Also, in Eq. (71) the complicated source term has been approximated by

$$\overline{f(\psi, Z)} = f(\overline{\psi}, \overline{Z}). \tag{72}$$

Indeed, the diffusion terms or the gradient of the stresses, linked to the second order viscous terms are more likely to appear in low Reynolds number regions, their analytical expression would be almost intractable for practical applications. From a purely mathematical point of view, this approximation would be justified only for linear functions for which the second derivative term $\partial^2\bar{\chi}/\partial\Delta^2$ reduces to zero. But second order terms are multiplied by the laminar viscosity and thus are usually important only in some restricted regions of the flow like the near wall region. At this stage, it is worth mentioning an important physical interpretation. Considering that the material derivative $D\Delta/Dt$ includes both an advection mean value and an advection fluctuating part, there are two physical effects in action. The mean value advection is acting when the gradient of the cell size is parallel to the mean flow going across the interface while the fluctuating advection can be interpreted as turbulent diffusion due to large scales motions and is mainly acting when the gradient of the cell size is perpendicular to a near wall boundary, the mean flow going along the interface. So, this term does contain two physical effects.

D. Filtered Navier-Stokes equations with varying filters

The Navier-Stokes equations governing the detailed flow evolution are the starting point of the analysis

$$\frac{\partial u_j}{\partial x_j} = 0 \tag{73}$$

and

$$\frac{\partial u_i}{\partial t} + \frac{\partial}{\partial x_j}(u_i u_j) = -\frac{1}{\rho}\frac{\partial p}{\partial x_i} + \nu \frac{\partial^2 u_i}{\partial x_j \partial x_j}, \tag{74}$$

where in this equation, the variables u_i, p, and ν denote the velocity, the pressure, and the viscous molecular viscosity, respectively. The usual practice used in LES calculations consists in neglecting the commutation error and consequently to solve the equation of the filtered motion[36] without correction terms. As a first approximation as shown in the preceding section, we shall account for the commutation terms only in the material derivative. Using the functional operator (7), the equation of mass conservation becomes

$$\frac{\partial \bar{u}_j}{\partial x_j} - \beta_{x_j}(u_j) = 0, \tag{75}$$

where β_{x_j} is given by Eq. (8) for $\phi = u_i$. Using the functional operator (26) and expression (65), the filtered momentum equation takes the form as

$$\frac{\partial \bar{u}_i}{\partial t} + \frac{\partial \left(\bar{u}_i \bar{u}_j\right)}{\partial x_j} - \beta_T(u_i) = -\frac{1}{\rho}\frac{\partial \bar{p}}{\partial x_i} + \frac{1}{\rho}\beta_{x_i}(p) - \frac{\partial \tau_{ij}}{\partial x_j} + \nu \frac{\partial^2 \bar{u}_i}{\partial x_j \partial x_j}$$
$$-\nu \frac{\partial^2 \Delta}{\partial x_j \partial x_j}\frac{\partial \bar{u}_i}{\partial \Delta} - \nu \frac{\partial \Delta}{\partial x_j}\frac{\partial \Delta}{\partial x_j}\frac{\partial^2 \bar{u}_i}{\partial \Delta^2} - 2\nu \frac{\partial \Delta}{\partial x_j}\frac{\partial^2 \bar{u}_i}{\partial x_j \partial \Delta}, \tag{76}$$

where $\beta_T(u_i)$ is given by Eq. (22) for $\phi = u_i$ leading to

$$\beta_T(u_i) = \frac{\partial \Delta}{\partial t}\frac{\partial \bar{u}_i}{\partial \Delta} + \frac{\partial \Delta}{\partial x_j}\frac{\partial (\overline{u_j u_i})}{\partial \Delta} = \frac{\partial \Delta}{\partial t}\frac{\partial \bar{u}_i}{\partial \Delta} + \frac{\partial \Delta}{\partial x_j}\left[\bar{u}_i \frac{\partial \bar{u}_j}{\partial \Delta} + \bar{u}_j \frac{\partial \bar{u}_i}{\partial \Delta} + \frac{\partial \tau(u_i, u_j)}{\partial \Delta}\right] \tag{77}$$

and with

$$\beta_{x_j}(p) = \frac{\partial \Delta}{\partial x_j}\frac{\partial \overline{p}}{\partial \Delta}, \tag{78}$$

if using the approximations detailed in the Sec. III C 4, the result is

$$\frac{\partial \bar{u}_i}{\partial t} + \frac{\partial (\bar{u}_i \bar{u}_j)}{\partial x_j} - \beta_T(u_i) = -\frac{1}{\rho}\frac{\partial \bar{p}}{\partial x_i} + \nu \frac{\partial^2 \bar{u}_i}{\partial x_j \partial x_j} - \frac{\partial \tau_{ij}}{\partial x_j}, \tag{79}$$

in which we shall use the more easily tractable approximate equation

$$\beta_T(u_i) \approx \frac{\partial \Delta}{\partial t}\frac{\partial \bar{u}_i}{\partial \Delta} + \bar{u}_j \frac{\partial \Delta}{\partial x_j}\frac{\partial \bar{u}_i}{\partial \Delta} = \frac{D\Delta}{Dt}\frac{\partial \bar{u}_i}{\partial \Delta}, \tag{80}$$

which corresponds to the approximations introduced in Eq. (71). At this step, we recall that the aim of the present paper is not to analyze the commutation errors in a general scope of large eddy simulations but only to devise a practical mean to account for variable filters or meshes in computational hybrid RANS-LES PITM simulations. With the aim to conduct the analytical developments in the following, we will also neglect systematically the commutation error appearing in the continuity equation (75). Indeed, strictly speaking, the filtered velocity field would not be exactly divergence free. We have supposed that the non-commutation terms in the material derivative (80) are of primary importance on the practical point of view for real flow simulations.

E. Numerical estimate of extra terms arising from the non-commutativity

After having chosen the adequate form of the filtered transport equations including simplified (or not) commutation terms, the present section deals with numerical approximations. Indeed, Eq. (80) can be written for any quantity ϕ to give

$$\beta_T(\phi) \approx \frac{\partial \Delta}{\partial t}\frac{\partial \overline{\phi}}{\partial \Delta} + \overline{u}_j \frac{\partial \Delta}{\partial x_j}\frac{\partial \overline{\phi}}{\partial \Delta} = \frac{D\Delta}{Dt}\frac{\partial \overline{\phi}}{\partial \Delta}. \tag{81}$$

At this stage, it is necessary to introduce a numerical mean to approximate the derivatives in Δ such as $\partial\overline{\phi}/\partial\Delta$ appearing in the commutation terms that can be used in practice during the simulations. To do this, we propose to apply a second filtering operation, with a larger width, like in the work of Iovieno and Tordella.[14] More precisely, whatever the variable ϕ,

$$\frac{\partial \bar{\phi}}{\partial \Delta} \approx \frac{\widetilde{\bar{\phi}} - \bar{\phi}}{\widetilde{\Delta} - \Delta}, \tag{82}$$

where $\widetilde{\bar{\phi}}$ denotes the twice filtered variable and $\widetilde{\Delta}$ the width of the superfilter. In practice, $\widetilde{\Delta} = 2\Delta$. The velocity $\widetilde{\bar{u}}_i$ field can be obtained by applying the superfilter to the currently calculated resolved solution at each time step of the calculation. As a result, β_T is computed as

$$\beta_T(u_i) \approx \frac{D\Delta}{Dt}\left(\frac{\widetilde{\bar{u}}_i - \bar{u}_i}{\widetilde{\Delta} - \Delta}\right). \tag{83}$$

Of course, if necessary the practitioner remains free to use a more complete approximation like

$$\beta_T(u_i) = \frac{\partial \Delta}{\partial t}\left(\frac{\widetilde{\bar{u}}_i - \bar{u}_i}{\widetilde{\Delta} - \Delta}\right) + \frac{\partial \Delta}{\partial x_j}\left[\bar{u}_j\left(\frac{\widetilde{\bar{u}}_i - \bar{u}_i}{\widetilde{\Delta} - \Delta}\right) + \bar{u}_i\left(\frac{\widetilde{\bar{u}}_j - \bar{u}_j}{\widetilde{\Delta} - \Delta}\right) + \left(\frac{\widetilde{\tau}(u_j, u_i) - \tau(u_j, u_i)}{\widetilde{\Delta} - \Delta}\right)\right]. \tag{84}$$

But the calculation will be heavier. Equation (82) is directly transposable in the spectral space by substituting Δ to κ_c and $\widetilde{\Delta}$ to $\widetilde{\kappa_c} = \kappa_c/2$.

IV. PITM EXTENSION METHOD FOR VARIABLE FILTERS

A. Subfilter scale stress transport equation

As it was mentioned in the Introduction, the PITM method allows to perform continuous hybrid non-zonal RANS-LES simulations with seamless coupling between RANS and LES regions. This method is particularly relevant for simulating flows on coarse meshes or flows that depart from the Kolmogorov equilibrium law. The main ingredient of this method is the new dissipation-rate equation[6] that constitutes the cornerstone of the modeling. This equation must be used in conjunction with the transport equation of the subfilter scale turbulent energy in the framework of first order closure[6] or the subfilter scale stress in the framework of second moment closure[7] (SMC). In this section, we will establish the transport equation of the subfilter scale stress tensor when applying variable filters taking into account the main part of the commutation terms. With the aim to obtain tractable equations, some approximations will be however conceded in the computations of the derivatives involving the turbulent processes of diffusion, production, redistribution, and destruction terms. Only the convective term which plays a major role in the commutation errors will be treated in its exact form. The issue to address is then to compute the transport equation for the tensor $\tau_{ij} = \overline{u_i u_j} - \bar{u}_i \bar{u}_j$ which is composed of two terms. First, the transport equation for $u_i u_j$ is simply obtained by multiplying Eq. (74) by u_j and to add the transposed equation obtained by a change of indices leading to

$$\frac{d(u_i u_j)}{dt} = \frac{\partial (u_i u_j)}{\partial t} + \frac{\partial (u_i u_j u_k)}{\partial x_k} = -\frac{1}{\rho}\left(u_j \frac{\partial p}{\partial x_i} + u_i \frac{\partial p}{\partial x_j}\right) + \nu\left(u_j \frac{\partial^2 u_i}{\partial x_k \partial x_k} + u_i \frac{\partial^2 u_j}{\partial x_k \partial x_k}\right). \tag{85}$$

Then, we can apply the functional operator (26) with $\phi = u_i u_j$ for computing its filtered equation

$$\overline{\frac{d(u_i u_j)}{dt}} = \frac{d(\overline{u_i u_j})}{dt} + \frac{\partial \tau(u_k, u_i u_j)}{\partial x_k} - \beta_T(u_i u_j), \tag{86}$$

where $\tau(u_k, u_i u_j)$ is given by its definition (25) as

$$\tau(u_k, u_i u_j) = \overline{u_i u_j u_k} - \overline{u_i u_j}\,\bar{u}_k, \tag{87}$$

so that

$$\overline{\frac{d(u_i u_j)}{dt}} = \frac{\partial(\overline{u_i u_j})}{\partial t} + \frac{\partial(\overline{u_i u_j}\,\bar{u}_k)}{\partial x_k} + \frac{\partial(\overline{u_i u_j u_k} - \overline{u_i u_j}\,\bar{u}_k)}{\partial x_k} - \beta_T(u_i u_j). \tag{88}$$

The filtering of Eq. (85) using Eq. (88) allows then to obtain the transport equation of the filtered tensor $\overline{u_i u_j}$ that reads

$$\frac{\partial(\overline{u_i u_j})}{\partial t} + \frac{\partial(\overline{u_i u_j}\bar{u}_k)}{\partial x_k} - \beta_T(u_i u_j) = -\frac{1}{\rho}\left(\overline{u_j \frac{\partial p}{\partial x_i}} + \overline{u_i \frac{\partial p}{\partial x_j}}\right)$$
$$+\nu\left(\overline{u_j \frac{\partial^2 u_i}{\partial x_k \partial x_k}} + \overline{u_i \frac{\partial^2 u_j}{\partial x_k \partial x_k}}\right) - \frac{\partial}{\partial x_k}\left(\overline{u_i u_j u_k} - \overline{u_i u_j}\,\bar{u}_k\right). \tag{89}$$

The transport equation for the quantity $\bar{u}_i \bar{u}_j$ is obtained by multiplying Eq. (79) by $\bar{u}_j$ and adding the transposed equation

$$\frac{\partial(\bar{u}_i \bar{u}_j)}{\partial t} + \frac{\partial(\bar{u}_i \bar{u}_j \bar{u}_k)}{\partial x_k} - \bar{u}_j \beta_T(u_i) - \bar{u}_i \beta_T(u_j) = -\frac{1}{\rho}\left(\bar{u}_j \frac{\partial \bar{p}}{\partial x_i} + \bar{u}_i \frac{\partial \bar{p}}{\partial x_j}\right)$$
$$+\nu\left(\bar{u}_j \frac{\partial^2 \bar{u}_i}{\partial x_k \partial x_k} + \bar{u}_i \frac{\partial^2 \bar{u}_j}{\partial x_k \partial x_k}\right) - \bar{u}_j \frac{\partial \tau_{ik}}{\partial x_k} - \bar{u}_i \frac{\partial \tau_{jk}}{\partial x_k}. \tag{90}$$

The transport equation of τ_{ij} is then obtained by subtracting Eq. (90) from Eq. (89) leading to

$$\frac{\partial \tau_{ij}}{\partial t} + \frac{\partial(\tau_{ij}\bar{u}_k)}{\partial x_k} - \beta_T(u_i u_j) + \bar{u}_j \beta_T(u_i) + \bar{u}_i \beta_T(u_j)$$
$$= -\frac{1}{\rho}\left(\overline{u_j \frac{\partial p}{\partial x_i}} + \overline{u_i \frac{\partial p}{\partial x_j}} - \bar{u}_j \frac{\partial \bar{p}}{\partial x_i} - \bar{u}_i \frac{\partial \bar{p}}{\partial x_j}\right)$$
$$+\nu\left(\overline{u_j \frac{\partial^2 u_i}{\partial x_k \partial x_k}} + \overline{u_i \frac{\partial^2 u_j}{\partial x_k \partial x_k}} - \bar{u}_j \frac{\partial^2 \bar{u}_i}{\partial x_k \partial x_k} - \bar{u}_i \frac{\partial^2 \bar{u}_j}{\partial x_k \partial x_k}\right)$$
$$-\frac{\partial}{\partial x_k}\left(\overline{u_i u_j u_k} - \overline{u_i u_j}\,\bar{u}_k\right) + \bar{u}_j \frac{\partial \tau_{ik}}{\partial x_k} + \bar{u}_i \frac{\partial \tau_{jk}}{\partial x_k}. \tag{91}$$

Taking into account that

$$\overline{u_i u_j u_k} - \overline{u_i u_j}\,\bar{u}_k = \overline{u_i u_j u_k} - \bar{u}_k \tau_{ij} - \bar{u}_i \bar{u}_j \bar{u}_k \tag{92}$$

and that

$$u_j \frac{\partial^2 u_i}{\partial x_k \partial x_k} + u_i \frac{\partial^2 u_j}{\partial x_k \partial x_k} = \frac{\partial^2 (u_i u_j)}{\partial x_k \partial x_k} - 2\frac{\partial u_i}{\partial x_k}\frac{\partial u_j}{\partial x_k}, \tag{93}$$

Eq. (91) can be finally rewritten in the generic form as

$$\frac{\partial \tau(u_i, u_j)}{\partial t} + \frac{\partial}{\partial x_k}\left(\tau(u_i, u_j)\bar{u}_k\right) - \beta_T(u_i u_j) + \bar{u}_j \beta_T(u_i) + \bar{u}_i \beta_T(u_j)$$
$$= -\frac{\partial \tau(u_i, u_j, u_k)}{\partial x_k} + \nu \frac{\partial^2 \tau(u_i, u_j)}{\partial x_k \partial x_k} - \frac{1}{\rho}\frac{\partial \tau(p, u_i)}{\partial x_j} - \frac{1}{\rho}\frac{\partial \tau(p, u_j)}{\partial x_i} + \tau\left(p, \frac{\partial u_i}{\partial x_j} + \frac{\partial u_j}{\partial x_i}\right)$$
$$-2\nu\tau\left(\frac{\partial u_i}{\partial x_k}, \frac{\partial u_j}{\partial x_k}\right) - \tau(u_i, u_k)\frac{\partial \bar{u}_j}{\partial x_k} - \tau(u_j, u_k)\frac{\partial \bar{u}_i}{\partial x_k}, \tag{94}$$

with the general definition

$$\tau(f, g) = \overline{fg} - \bar{f}\bar{g} \tag{95}$$

and

$$\tau(f, g, h) = \overline{fgh} - \bar{f}\tau(g, h) - \bar{g}\tau(h, f) - \bar{h}\tau(f, g) - \bar{f}\bar{g}\bar{h}, \tag{96}$$

for any turbulent quantities f, g, h. As a result of interest, one can see that Eq. (94) takes the same form as Eq. (22) in Ref. 38 written in term of general moments[38,39] apart from the additional terms $\beta_T(u_iu_j)$, $\bar{u}_i\beta_T(u_i)$, and $\bar{u}_j\beta_T(u_j)$ appearing in the left hand side of this equation arising from the commutation errors involved in the convective process. The commutation term can be developed using Eq. (22) for evaluating β_T as follows:

$$\beta_T(u_i u_j) - \bar{u}_j \beta_T(u_i) - \bar{u}_i \beta_T(u_j) = \frac{\partial \Delta}{\partial t}\frac{\partial(\overline{u_i u_j})}{\partial \Delta} + \frac{\partial \Delta}{\partial x_k}\frac{\partial(\overline{u_k u_i u_j})}{\partial \Delta}$$
$$-\bar{u}_j\left[\frac{\partial \Delta}{\partial t}\frac{\partial \bar{u}_i}{\partial \Delta} + \frac{\partial \Delta}{\partial x_k}\frac{\partial(\overline{u_k u_i})}{\partial \Delta}\right] - \bar{u}_i\left[\frac{\partial \Delta}{\partial t}\frac{\partial \bar{u}_j}{\partial \Delta} + \frac{\partial \Delta}{\partial x_k}\frac{\partial(\overline{u_k u_j})}{\partial \Delta}\right], \tag{97}$$

which can be rewritten as

$$\beta_T(u_i u_j) - \bar{u}_j \beta_T(u_i) - \bar{u}_i \beta_T(u_j) = \frac{\partial \Delta}{\partial t}\frac{\partial \tau(u_i, u_j)}{\partial \Delta} + \frac{\partial \Delta}{\partial x_k}\left[\frac{\partial(\overline{u_k u_i u_j})}{\partial \Delta} - \bar{u}_j\frac{\partial(\overline{u_k u_i})}{\partial \Delta} - \bar{u}_i\frac{\partial(\overline{u_k u_j})}{\partial \Delta}\right]. \tag{98}$$

The simplified and more tractable form of these equations can be derived easily, using Eq. (96), as detailed in the following. We need first to rewrite Eq. (98) in a more practical form considering the correlation tensor $\tau(u_i, u_j, u_k)$ instead of $\overline{u_i u_j u_k}$. Using the relation defined in Eq. (96) taken for u_i, u_j, and u_k as

$$\tau(u_i, u_j, u_k) = \overline{u_i u_j u_k} - \bar{u}_i\tau(u_j, u_k) - \bar{u}_j\tau(u_i, u_k) - \bar{u}_k\tau(u_i, u_j) - \bar{u}_i\bar{u}_j\bar{u}_k, \tag{99}$$

one can easily find that Eq. (98) transforms into

$$\beta_T(u_i u_j) - \bar{u}_j \beta_T(u_i) - \bar{u}_i \beta_T(u_j) = \frac{\partial \Delta}{\partial t}\frac{\partial \tau(u_i, u_j)}{\partial \Delta} + \frac{\partial \Delta}{\partial x_k}\left[\frac{\partial \tau(u_i, u_j, u_k)}{\partial \Delta}\right.$$
$$\left. + \tau(u_j, u_k)\frac{\partial \bar{u}_i}{\partial \Delta} + \tau(u_i, u_k)\frac{\partial \bar{u}_j}{\partial \Delta} + \tau(u_i, u_j)\frac{\partial \bar{u}_k}{\partial \Delta} + \bar{u}_k\frac{\partial \tau(u_i, u_j)}{\partial \Delta} - \bar{u}_i\bar{u}_j\frac{\partial \bar{u}_k}{\partial \Delta}\right]. \tag{100}$$

This equation is of very complex form. In the first approximation, we will retain only the convective term associated with the spatial derivative $\partial\Delta/\partial x_k$. In this case, $\beta_T(u_i u_j) - \bar{u}_j\beta_T(u_i) + \bar{u}_i\beta_T(u_j)$ takes the simple form as follows:

$$\beta_T(u_i u_j) - \bar{u}_j \beta_T(u_i) - \bar{u}_i \beta_T(u_j) \approx \left(\frac{\partial(\overline{u_i u_j})}{\partial \Delta} - \bar{u}_j\frac{\partial \bar{u}_i}{\partial \Delta} - \bar{u}_i\frac{\partial \bar{u}_j}{\partial \Delta}\right)\frac{D\Delta}{Dt} = \frac{\partial \tau(u_i, u_j)}{\partial \Delta}\frac{D\Delta}{Dt}. \tag{101}$$

The subfilter turbulent energy is obtained by the tensor contraction of the subfilter scale stress tensor $\tau(u_i, u_j)$ as

$$k_{sfs} = \frac{1}{2}\tau(u_j u_j), \tag{102}$$

$$\frac{\partial k_{sfs}}{\partial t} + \frac{\partial}{\partial x_k}\left(k_{sfs}\bar{u}_k\right) - \frac{1}{2}\beta_T(u_i u_i) + \bar{u}_i\beta_T(u_i)$$
$$= -\frac{1}{2}\frac{\partial \tau(u_i, u_i, u_k)}{\partial x_k} + \nu\frac{\partial^2 k_{sfs}}{\partial x_k \partial x_k} - \nu\tau\left(\frac{\partial u_i}{\partial x_k}, \frac{\partial u_i}{\partial x_k}\right) - \tau(u_i, u_k)\frac{\partial \bar{u}_i}{\partial x_k}, \tag{103}$$

with also for the turbulence energy commutation terms

$$\frac{1}{2}\beta_T(u_i u_i) - \bar{u}_i\beta_T(u_i) = \frac{\partial \Delta}{\partial t}\frac{\partial k_{sfs}}{\partial \Delta} + \frac{\partial \Delta}{\partial x_k}\left[\frac{\partial(\overline{u_k u_i u_i})}{\partial \Delta} - \bar{u}_i\frac{\partial(\overline{u_k u_i})}{\partial \Delta}\right]. \tag{104}$$

The simplified and more tractable form of the equation can be obtained as previously,

$$\frac{1}{2}\beta_T(u_i u_i) - \bar{u}_i\beta_T(u_i) \approx \frac{\partial k_{sfs}}{\partial \Delta}\frac{D\Delta}{Dt} \tag{105}$$

equation which is nothing more than the tensorial contraction of Eq. (101). The approximations (101) and (105) have the advantage to remain in perfect correspondence and physical interpretation with the statistical equations with variable splitting.

B. Practical numerical estimate of extra-terms in subfilter turbulence equations

We again consider the numerical approximation of derivatives in Δ appearing in the commutation terms of the turbulence equations. According to the developments made in Sec. III E referring to Eq. (82), the use of a superfilter allows to approximate the commutation term $\beta_T(u_i u_j) - \bar{u}_j\beta_T(u_i) + \bar{u}_i\beta_T(u_j)$ defined in Eq. (98) which is computed using a superfilter as

$$\beta_T(u_i u_j) - \bar{u}_j\beta_T(u_i) - \bar{u}_i\beta_T(u_j) = \frac{D\Delta}{Dt}\left(\frac{\widetilde{\tau}(u_i, u_j) - \tau(u_i, u_j)}{\widetilde{\Delta} - \Delta}\right) \tag{106}$$

and for the turbulence energy, like for Eq. (106)

$$\frac{1}{2}\beta_T(u_i u_i) - \bar{u}_i\beta_T(u_i) = \frac{D\Delta}{Dt}\left(\frac{\widetilde{k_{sfs}} - k_{sfs}}{\widetilde{\Delta} - \Delta}\right). \tag{107}$$

These estimates are consistent with the approximations used in the momentum equation. Physically, the amount of energy gain or lost in the resolved scales due to filter width variation is, respectively, exactly compensated by an energy lost or gain in the subfilter turbulence equations.

C. Subfilter scale dissipation-rate transport equation

The derivation of the dissipation rate equation is the core of the PITM method. It has been fully described for the first time in Ref. 6 using a partial integration procedure applied to the energy equation in the spectral space involving the wave number ranges [0, κ_c], [κ_c, κ_d], and [κ_d, ∞[where κ_c is the cutoff wave number whereas κ_d is a very large wave number located just before the dissipation range of the energy spectrum. The same concept has been afterward introduced in Refs. 7, 40, and 41 for stress transport modeling. As a result of the modeling developed first in homogeneous flows in the statistical sense and then extended to non-homogeneous flows using the concept of tangent homogeneous field,[36] the dissipation rate equation reads

$$\frac{\partial \epsilon_{sfs}}{\partial t} = c_{sfs\epsilon_1}\frac{\epsilon_{sfs}}{k_{sfs}}P - c_{sfs\epsilon_2}\frac{\epsilon_{sfs}^2}{k_{sfs}}, \tag{108}$$

where $c_{sfs\epsilon_1} = 3/2$ and

$$c_{sfs\epsilon_2} = \frac{\langle k_{sfs}\rangle}{\kappa_d E(\kappa_d)}\left[\frac{\mathcal{F}(\kappa_d) - F(\kappa_d)}{\langle \epsilon_{sfs}\rangle}\right]. \tag{109}$$

In Eq. (108), P denotes the production term of the subfilter turbulent energy given by

$$P = -\tau(u_i, u_k)\frac{\partial \bar{u}_j}{\partial x_k}, \tag{110}$$

while in Eq. (109), $\mathcal{F}(\kappa_d)$ is the spectral transfer at this location and $F(\kappa_d)$ is the gross flux at the splitting wave number defined by

$$F(\kappa_d) = \mathcal{F}(\kappa_d) + E(\kappa_d)\frac{\partial \kappa_d}{\partial t}. \tag{111}$$

Further analytical developments made in Ref. 41 have shown then that the coefficient $c_{sfs\epsilon_1}$ appearing in the production term is not necessary equal to 3/2 but can take on its corresponding RANS value $c_{sfs\epsilon_1} = c_{\epsilon_1}$ whatever the value used in the statistical dissipation-rate equation. The derivation of the method was originally carried out for constant or slow varying filter cutoff κ_c. Although this hypothesis was not formally used in the mathematical development, unless to assume that κ_c still remains much lower than the dissipative wave number κ_d which evolves itself in time and space, nothing has to be changed when the cutoff wave number varies rapidly. This assertion can be intuitively understood. In the case where κ_c is strongly varying in time and space, the flux $F(\kappa_c)$ will be modified due to the splitting variation according to equation

$$F(\kappa_c) = \mathcal{F}(\kappa_c) + E(\kappa_c)\frac{\partial \kappa_c}{\partial t} \tag{112}$$

showing that a part of the energy fed into the modeled range is due to the variation in splitting wave number. But the spectrum itself does not change at all, just the splitting is changing, so that there is no reason for the dissipation rate to be modified. From a physical point of view, this outcome simply means that the dissipation-rate ϵ indeed interpreted as the energy flux $F(\kappa_d)$ passing through the dissipative wave number κ_d remains unaffected by the location of the cutoff wave number $\kappa_c = \pi/\Delta$. Indeed, we know that the PITM method is fully consistent with the concept of inertial cascade.[6] From a practical point of view, Eq. (108) needs to be closed. Further developments have shown that the coefficient $c_{sfs\epsilon_2}$ is a linear function of the ratio of the subfilter energy to the total energy k_{sfs}/k as follows:[6,7]

$$c_{\epsilon_{sfs2}} = c_{\epsilon_1} + \frac{\langle k_{sfs}\rangle}{k}\left(c_{\epsilon_2} - \frac{3}{2}\right), \tag{113}$$

whatever the c_{ϵ_1} and c_{ϵ_2} values used in RANS modeling.[41] The ratio $<k_{sfs}>/k$ is evaluated as a function of the dimensionless parameter η_c

$$\eta_c = \kappa_c L_e = \frac{\pi L_e}{\Delta} \tag{114}$$

involving the cutoff wave number κ_c and the turbulent length scale L_e

$$L_e = \frac{k^{3/2}}{\langle\epsilon_{sfs}\rangle + \langle\epsilon^<\rangle}, \tag{115}$$

built using the total turbulent kinetic energy k and the total dissipation composed of the subfilter dissipation rate ϵ_{sfs} given by its transport equation and the large scale dissipation rate denoted $\epsilon^<$ calculated explicitly by

$$\epsilon^< = \nu\,\overline{\frac{\partial u_i^<}{\partial x_j}\frac{\partial u_i^<}{\partial x_j}}. \tag{116}$$

In Eq. (114), the quantity Δ is the effective filter accounting for the anisotropy of the grid near the walls like the proposal of Scotti[42]

$$\Delta = \Delta_a\left(\zeta + (1-\zeta)\frac{\Delta_b}{\Delta_a}\right), \tag{117}$$

where the filters Δ_a and Δ_b are defined by $\Delta_a = (\Delta_1\Delta_2\Delta_3)^{1/3}$ and $\Delta_b = (\Delta_1^2 + \Delta_2^2 + \Delta_3^2)/3)^{1/2}$ and where ζ is a constant parameter. Note that in PITM methodology, the model varies continuously with respect to the ratio of the turbulent length-scale to the grid-size L_e/Δ. If we have inferred that no modification is necessary in the dissipation rate equation for variable filters, it can be pointed out, however, that the production term itself defined in Eq. (110) will be indirectly modified.

V. PITM METHOD WITH VARIABLE FILTERS IN PRACTICE

The purpose of this section is to provide for practitioners in CFD the practical recapitulate of the subfilter scale models which need to be used when variable filters are taken into account in the equations governing turbulent flows.

A. Navier-Stokes equations

Using the approximations developed above, the mass conservation equation (75) and the resolved scale equation of motion (79) to be solved are finally for the mass conservation

$$\frac{\partial \bar{u}_j}{\partial x_j} + \frac{\partial \Delta}{\partial x_j}\frac{\partial \bar{u}_j}{\partial \Delta} = 0, \tag{118}$$

and using the functional operator (26), for the filtered momentum equation

$$\frac{\partial \bar{u}_i}{\partial t} + \frac{\partial (\bar{u}_i \bar{u}_j)}{\partial x_j} = \frac{\partial \Delta}{\partial t}\frac{\partial \bar{u}_i}{\partial \Delta} + \frac{\partial \Delta}{\partial x_j}\frac{\partial (\bar{u}_i \bar{u}_j)}{\partial \Delta} - \frac{1}{\rho}\frac{\partial \bar{p}}{\partial x_i} + \nu \frac{\partial^2 \bar{u}_i}{\partial x_j \partial x_j} - \frac{\partial \tau_{ij}}{\partial x_j}, \tag{119}$$

but the approximate form of this equation is retained in practices as follows:

$$\frac{\partial \bar{u}_i}{\partial t} + \frac{\partial (\bar{u}_i \bar{u}_j)}{\partial x_j} = \frac{\partial \bar{u}_i}{\partial \Delta}\frac{D\Delta}{Dt} - \frac{1}{\rho}\frac{\partial \bar{p}}{\partial x_i} + \nu \frac{\partial^2 \bar{u}_i}{\partial x_j \partial x_j} - \frac{\partial \tau_{ij}}{\partial x_j}, \tag{120}$$

with

$$\frac{\partial \bar{u}_i}{\partial \Delta} \approx \frac{\widetilde{\bar{u}}_i - \bar{u}_i}{\widetilde{\Delta} - \Delta}. \tag{121}$$

B. Subfilter scale viscosity models

In the case of subfilter scale viscosity models, the subfilter-scale stress energy τ_{ij} appearing in the left-hand side of Eq. (120) is modeled by means of the Boussinesq hypothesis, nonlinear model or even algebraic stress model taking into account an eddy viscosity. The Boussinesq hypothesis leads to the well known relation

$$\tau_{ij} = -\nu_{sfs}\left(\frac{\partial \bar{u}_i}{\partial x_j} + \frac{\partial \bar{u}_j}{\partial x_i}\right) + \frac{2}{3}k_{sfs}\delta_{ij}, \tag{122}$$

where the eddy viscosity ν_{sfs} reads[6]

$$\nu_{sfs} = c_\mu \frac{k_{sfs}^2}{\epsilon_{sfs}} \tag{123}$$

and where c_μ is a constant coefficient. In Eq. (122), the subfilter scale turbulent energy and dissipation-rate are computed by their own transport equations (103) and (108), modeled, respectively, as

$$\frac{\partial k_{sfs}}{\partial t} + \frac{\partial}{\partial x_k}\left(k_{sfs}\bar{u}_k\right) = P + \frac{D\Delta}{Dt}\frac{\partial k_{sfs}}{\partial \Delta} - \epsilon_{sfs} + J \tag{124}$$

and

$$\frac{\partial \epsilon_{sfs}}{\partial t} + \frac{\partial}{\partial x_k}\left(\epsilon_{sfs}\bar{u}_k\right) = c_{sfs\epsilon_1}\frac{\epsilon_{sfs}}{k_{sfs}}\left[P + \frac{D\Delta}{Dt}\frac{\partial k_{sfs}}{\partial \Delta}\right] - c_{sfs\epsilon_2}\frac{\epsilon_{sfs}^2}{k_{sfs}} + J_\epsilon, \tag{125}$$

and where the turbulence diffusion terms J and J_ϵ have been embedded into these equations in the general case of inhomogeneous flows. These terms are modeled using a gradient law hypothesis

$$J = \frac{\partial}{\partial x_j}\left[\left(\nu + \frac{\nu_{sfs}}{\sigma_k}\right)\frac{\partial k_{sfs}}{\partial x_j}\right] \tag{126}$$

and

$$J_\epsilon = \frac{\partial}{\partial x_j}\left[\left(\nu + \frac{\nu_{sfs}}{\sigma_\epsilon}\right)\frac{\partial \epsilon_{sfs}}{\partial x_j}\right], \tag{127}$$

where σ_k and σ_ϵ are constant coefficients. In low Reynolds number flows, additional correction terms may also appear in Eq. (125), but they are not detailed here. Note that the commutation term arising from the convective term of the subfilter turbulent energy appearing in Eq. (124) has been included in Eq. (125) as an additional production term. This practice becomes obvious if one refers to the technique of derivation of the dissipation rate equation in the PITM method that makes use of the kinetic energy equation (see Eqs. (10) and (11) on p. 448 of Ref. 6). This technique allows for instance to keep a time scale equation in a homogeneous turbulence field that takes the form

$$\frac{\partial}{\partial t}\left(\frac{k_{sfs}}{\epsilon_{sfs}}\right) = \frac{\epsilon_{sfs}}{k_{sfs}^2}\left[\left(P + \frac{D\Delta}{Dt}\frac{\partial k_{sfs}}{\partial \Delta}\right)(c_{sfs\epsilon_1} - 1) - \epsilon(c_{sfs\epsilon_2} - 1)\right] \tag{128}$$

and so, the usual equilibrium value for the ratio of the production P including the additional filtering term to the dissipation

$$\frac{1}{\epsilon}\left(P + \frac{D\Delta}{Dt}\frac{\partial k_{sfs}}{\partial \Delta}\right) \rightarrow \frac{c_{sfs\epsilon_2} - 1}{c_{sfs\epsilon_1} - 1} \tag{129}$$

is thus preserved.

C. Subfilter scale stress models

In the second moment closure (SMC), the subfilter scale stress transport equation deduced from Eq. (94) is directly derived as

$$\frac{\partial \tau_{ij}}{\partial t} + \frac{\partial}{\partial x_k}(\tau_{ij}\bar{u}_k) = P_{ij} + \frac{D\Delta}{Dt}\frac{\partial \tau_{ij}}{\partial \Delta} + \Pi_{ij} - \frac{2}{3}\delta_{ij}\epsilon_{sfs} + J_{ij}. \tag{130}$$

In this equation, the production term P_{ij} takes on the exact expression

$$P_{ij} = -\tau_{ik}\frac{\partial \bar{u}_j}{\partial x_k} - \tau_{jk}\frac{\partial \bar{u}_i}{\partial x_k}. \tag{131}$$

The redistribution term Π_{ij} is usually decomposed into a slow part Π^1_{ij} which characterizes the return to isotropy due to the action of turbulence on itself and a rapid part Π^2_{ij} which describes the return to isotropy by action of the filtered velocity gradient. These terms can be modeled for instance as made in Refs. 7 and 43

$$\Pi^1_{ij} = -c_{sfs_1}\frac{\epsilon_{sfs}}{k_{sfs}}\left(\tau_{ij} - \frac{2}{3}k_{sfs}\,\delta_{ij}\right). \tag{132}$$

In Eq. (132), c_1 is the Rotta coefficient modified to account for the spectrum splitting.[43] The second term Π^2_{ij} can be modeled by means of the rapid distortion theory (RDT) for homogeneous strained turbulence in an initially isotropic state[7,44]

$$\Pi^2_{ij} = -c_2\left(P_{ij} - \frac{1}{3}P_{mm}\delta_{ij}\right), \tag{133}$$

where the coefficient c_2 remains the same as in statistical modeling. The diffusion term J_{ij} appearing in Eq. (130) associated with the fluctuating velocities and pressure together with the molecular diffusion is modeled assuming a well known gradient law hypothesis

$$J_{ij} = \frac{\partial}{\partial x_k}\left(\nu \frac{\partial \tau_{ij}}{\partial x_k} + c_s \frac{k_{sfs}}{\epsilon_{sfs}} \tau_{kl} \frac{\partial \tau_{ij}}{\partial x_l}\right), \tag{134}$$

where c_s is a constant numerical coefficient. The subfilter scale dissipation-rate ϵ_{sfs} appearing in Eq. (130) is still computed from its modeled transport equation (125) but the diffusion term involves now a tensorial eddy viscosity concept as follows:

$$J_{\epsilon} = \frac{\partial}{\partial x_j}\left(\nu \frac{\partial \epsilon_{sfs}}{\partial x_j} + c_{\epsilon} \frac{k_{sfs}}{\epsilon_{sfs}} \tau_{jm} \frac{\partial \epsilon_{sfs}}{\partial x_m}\right), \tag{135}$$

where the coefficient c_ϵ remains constant. The coefficients used in these energy and stress subfilter models can be found in Refs. 6, 43, 45, and 46. In this section, all the additional commutation terms have been expressed using the filter Δ. Of course, it is also possible to introduce the cutoff wave number κ_c in place of Δ in the modeled transport equations (127), (128), and (130). However, considering that the variation of the subfilter scale stress τ_{ij} as a function of κ_c is very probably nonlinear, it may be worth considering the option of an improved approximation deduced from the energy spectrum as shown in Subsection A 5 of the Appendix. The impact of these correction terms in practical calculations can be discussed with the following remark in mind. The commutation terms approximations such as

$$C = \frac{D\Delta}{Dt}\frac{\partial \phi}{\partial \Delta} \tag{136}$$

appearing in Eqs. (124), (125), and (130) can be written as

$$C = \left(\frac{\partial \Delta}{\partial t} + \bar{u}_j \frac{\partial \Delta}{\partial x_j}\right)\frac{\partial \phi}{\partial \Delta} = \frac{\partial \Delta}{\partial t}\frac{\partial \phi}{\partial \Delta} + \langle u_j \rangle \frac{\partial \Delta}{\partial x_j}\frac{\partial \phi}{\partial \Delta} + u_j^{<} \frac{\partial \Delta}{\partial x_j}\frac{\partial \phi}{\partial \Delta}. \tag{137}$$

As a result, it is of interest to note that the first term in the right hand side of Eq. (137) acts in time varying flows, the second term acts in space when the filter size varies in the direction of the mean flow (crossing the interface) while the third term can act also when the filter size is varying in both directions, mean flow and perpendicular to the mean flow (flowing along the interface). The second term can be said to refer to the material derivative or a convection process whereas the third term can be said to refer to turbulent large scale turbulent diffusion, i.e., the diffusion due to the resolved scales.

VI. DECAY OF HOMOGENEOUS ISOTROPIC TURBULENCE

A. Generation of isotropic turbulence with an imposed spectrum energy subfilter scale stress models

With the aim to illustrate the theoretical development of the effect of varying filter width in time and space on the governing equations of mass, momentum, and turbulence model, and to show the usefulness of the proposed approach, we will perform here numerical simulations of isotropic decaying turbulence. This test case is indeed particularly appropriate for studying turbulence models in their capacity to mimic the Kolmogorov cascade process including the transfer of energy from the large scales to the small scale as well as the dissipation of the small scales by the molecular viscosity. For this application, we use the numerical code developed by Chaouat[47,48] based on the finite volume technique including a Runge-Kutta scheme of fourth-order accuracy in time with a combination of a quasi-centered scheme of fourth-order accuracy in space which has shown good numerical properties.[48] The initial mean velocity is zero and an analytical homogeneous random field[43,49] has been generated in a cubic box of size $L = N\Delta$ as initial condition with a given energy spectrum verifying

$$\langle \hat{u}_i(\boldsymbol{\kappa})\hat{u}_i(-\boldsymbol{\kappa})\rangle = \left(\frac{2\pi}{L}\right)^3 \frac{E(\kappa)}{2\pi\kappa^2}, \tag{138}$$

where $\hat{u}_i(\boldsymbol{\kappa})$ denotes the Fourier transform of the instantaneous velocity. The wave-numbers are defined by $\boldsymbol{\kappa} = 2\pi\,[m, n, p]^T/L$, where m, n, p are integers that vary from $-N/2+1$ to $N/2$ leading to a minimum wave-number $\kappa_{min} = 2\pi/(N\Delta)$ and a maximum wave-number $\kappa_{max} = \pi/\Delta$. The energy spectrum is defined by

$$E(\kappa) = \alpha\kappa^m \quad for \quad \kappa \leq \kappa_0,$$
$$E(\kappa) = C_\kappa\,\epsilon^{2/3}\,\kappa^{-5/3} \quad for \quad \kappa \geq \kappa_0, \tag{139}$$

where C_κ is the Kolmogorov constant. The maximum of the spectrum is obtained for κ_0 which is defined by the continuity of the two functions in Eq. (139)

$$\kappa_0 = \left(\frac{C_\kappa\epsilon^{2/3}}{\alpha}\right)^{\frac{3}{3m+5}}. \tag{140}$$

The subfilter and resolved parts of the turbulent energy are determined by integration of the spectrum. For the usual case where the cutoff wave number κ_c is located in the inertial zone of the spectrum implying $\kappa_c > \kappa_0$, the subfilter energy is then given by

$$\langle k_{sfs}\rangle = \int_{\kappa_c}^{\infty} E(\kappa)\,d\kappa = \frac{3}{2}C_\kappa\epsilon^{2/3}\kappa_c^{-2/3}, \tag{141}$$

whereas the total energy is

$$k = \int_0^{\infty} E(\kappa)\,d\kappa = \frac{3m+5}{2(m+1)}C_\kappa\epsilon^{2/3}\kappa_0^{-2/3} = \frac{3m+5}{2(m+1)}\,\alpha^{\frac{2}{3m+5}}\,C_\kappa^{\frac{3(m+1)}{3m+5}}\,\epsilon^{\frac{2(m+1)}{3m+5}} \tag{142}$$

leading to the ratio of the subfilter energy to the total energy

$$\frac{\langle k_{sfs}\rangle}{k} = \frac{3(m+1)}{3m+5}\left(\frac{\kappa_0}{\kappa_c}\right)^{2/3}. \tag{143}$$

The simulations are performed on the same mesh of dimension $L = 1.25$ m accounting $N = 80^3$ grid points for a medium cutoff wave number $\kappa_c = 2\ \mathrm{cm}^{-1}$. The equation describing the law of the dissipation-rate decay can be easily derived by taking the derivative of Eq. (142)

$$\frac{dk}{k} = \left(\frac{2m+2}{3m+5}\right)\frac{d\epsilon}{\epsilon} \tag{144}$$

and by considering the equation of the total turbulent energy decay,

$$\frac{dk}{dt} = -\epsilon, \tag{145}$$

one can finally get the resulting equation

$$\frac{d\epsilon}{dt} = -\left(\frac{3m+5}{2m+2}\right)\frac{\epsilon^2}{k} = -c_{\epsilon_2}\frac{\epsilon^2}{k}. \tag{146}$$

For the particular value $m = 1.4$, the present limiting value $lim_{\,\eta_c\to 0}\; c_{sfs\epsilon_2}(\eta_c) = c_{\epsilon_2} \approx 1.9$ is recovered.[6,37] These decay laws are supposing that the shape of the energy spectrum (139) remains unchanged during decay, this is not absolutely true so that the resulting Eq. (146) is only approximate. In the application considered here, the turbulent Reynolds number $R_t = k^2/\nu\epsilon$ based on the turbulent energy and the dissipation-rate is about 5000. For this case, the ratio value of the subfilter energy to the total energy is roughly 0.20 implying an appreciable part of subfilter turbulence energy.

B. Fixed grid

The equations to be solved are a particular case of the model given in the Sec. V B. Indeed it is not necessary to deal with stress transport equations in the present application for isotropic decaying turbulence. As usually, the filtered mass and motion equations to be solved are

$$\frac{\partial \bar{u}_j}{\partial x_j} = 0, \tag{147}$$

$$\frac{\partial \bar{u}_i}{\partial t} + \frac{\partial(\bar{u}_i \bar{u}_j)}{\partial x_j} = -\frac{1}{\rho}\frac{\partial \bar{p}}{\partial x_i} + \nu \frac{\partial^2 \bar{u}_i}{\partial x_j \partial x_j} - \frac{\partial \tau_{ij}}{\partial x_j}. \tag{148}$$

The subfilter stress τ_{ij} appearing in Eq. (148) is solved assuming a viscosity model defined in Eq. (123) where the subfilter scale and energy are solutions of the transport equations as follows:

$$\frac{\partial k_{sfs}}{\partial t} + \frac{\partial}{\partial x_k}\left(k_{sfs}\bar{u}_k\right) = P - \epsilon_{sfs} + \frac{\partial}{\partial x_j}\left[\left(\nu + \frac{\nu_{sfs}}{\sigma_k}\right)\frac{\partial k_{sfs}}{\partial x_j}\right] \tag{149}$$

and

$$\frac{\partial \epsilon_{sfs}}{\partial t} + \frac{\partial}{\partial x_k}\left(\epsilon_{sfs}\bar{u}_k\right) = c_{sfs\epsilon_1}\frac{\epsilon_{sfs}}{k_{sfs}}P - c_{sfs\epsilon_2}\frac{\epsilon_{sfs}^2}{k_{sfs}} + \frac{\partial}{\partial x_j}\left[\left(\nu + \frac{\nu_{sfs}}{\sigma_\epsilon}\right)\frac{\partial \epsilon_{sfs}}{\partial x_j}\right], \tag{150}$$

with

$$P = -\tau_{ij}\frac{\partial \bar{u}_i}{\partial x_j}. \tag{151}$$

C. Expanding grid without correction terms

The expanding grid is introduced by using a variable change. The inertial reference coordinate system x_j is replaced by a moving coordinate system ξ_j such that $\boldsymbol{\xi}(t, \boldsymbol{x}) = A(t)\boldsymbol{x}$ given by the transformation

$$\begin{cases} \vartheta = t \\ \xi_j = A(t)x_j \end{cases}, \tag{152}$$

with for derivatives

$$\begin{cases} \dfrac{\partial}{\partial t} = \dfrac{\partial}{\partial \vartheta}\dfrac{\partial \vartheta}{\partial t} + \dfrac{\partial}{\partial \xi_j}\dfrac{\partial \xi_j}{\partial t} = \dfrac{\partial}{\partial \vartheta} + \dfrac{\xi_j}{A(t)}\dfrac{dA(t)}{dt}\dfrac{\partial}{\partial \xi_j} \\ \dfrac{\partial}{\partial x_j} = \dfrac{\partial}{\partial \xi_j}\dfrac{\partial \xi_j}{\partial x_j} = A(t)\dfrac{\partial}{\partial \xi_j} \end{cases}. \tag{153}$$

This transformation is in fact a particular case of the Rogallo time-dependent linear transformation[50] which was used in numerical experiments on the structure of homogeneous turbulence performed by Lee and Reynolds.[51] Using the change of variables (152) with the derivative (153), the momentum equation then transforms as

$$\frac{\partial \bar{u}_i}{\partial \vartheta} + \frac{\xi_j}{A(\vartheta)}\frac{dA(\vartheta)}{d\vartheta}\frac{\partial \bar{u}_i}{\partial \xi_j} + A(\vartheta)\frac{\partial(\bar{u}_i\bar{u}_j)}{\partial \xi_j} = -\frac{A(\vartheta)}{\rho}\frac{\partial \bar{p}}{\partial \xi_i} + A^2(\vartheta)\nu\frac{\partial^2 \bar{u}_i}{\partial \xi_j \partial \xi_j} - A(\vartheta)\frac{\partial \tau_{ij}}{\partial \xi_j}, \tag{154}$$

whereas the continuity equation reads

$$\frac{\partial \bar{u}_j}{\partial \xi_j} = 0. \tag{155}$$

Considering the vector $V_i(\boldsymbol{\xi}, \vartheta)$ defined as

$$V_i(\boldsymbol{\xi}, \vartheta) = \frac{d}{d\vartheta}\left(\frac{\xi_i}{A(\vartheta)}\right) = -\frac{\xi_i}{A^2(\vartheta)}\frac{dA(\vartheta)}{d\vartheta}, \tag{156}$$

which can be interpreted as the local mesh velocity, Eq. (154) then can be rewritten into the compact form as

$$\frac{\partial \bar{u}_i}{\partial \vartheta} + A(\vartheta)\frac{\partial(\bar{u}_i\bar{u}_j)}{\partial \xi_j} - V_j A(\vartheta)\frac{\partial \bar{u}_i}{\partial \xi_j} = -\frac{A(\vartheta)}{\rho}\frac{\partial \bar{p}}{\partial \xi_i} + A^2(\vartheta)\nu\frac{\partial^2 \bar{u}_i}{\partial \xi_j \partial \xi_j} - A(\vartheta)\frac{\partial \tau_{ij}}{\partial \xi_j}. \tag{157}$$

Using the same procedure, the subfilter turbulent energy equation becomes

$$\frac{\partial k_{sfs}}{\partial \vartheta} + A(\vartheta)\frac{\partial}{\partial \xi_k}\left(k_{sfs}\bar{u}_k\right) - V_k A(\vartheta)\frac{\partial k_{sfs}}{\partial \xi_k} = P - \epsilon_{sfs} + A^2(\vartheta)\frac{\partial}{\partial \xi_j}\left[\left(\nu + \frac{\nu_{sfs}}{\sigma_k}\right)\frac{\partial k_{sfs}}{\partial \xi_j}\right], \tag{158}$$

where

$$P = -A(\vartheta)\tau_{ij}\frac{\partial \bar{u}_i}{\partial \xi_j}, \tag{159}$$

$$\tau_{ij} = -A(\vartheta)\nu_{sfs}\left(\frac{\partial \bar{u}_j}{\partial \xi_j} + \frac{\partial \bar{u}_i}{\partial \xi_j}\right) + \frac{2}{3}k_{sfs}\delta_{ij}, \tag{160}$$

and the subfilter scale dissipation rate reads

$$\frac{\partial \epsilon_{sfs}}{\partial \vartheta} + A(\vartheta)\frac{\partial}{\partial \xi_k}\left(\epsilon_{sfs}\bar{u}_k\right) - V_k A(\vartheta)\frac{\partial \epsilon_{sfs}}{\partial \xi_k} = c_{sfs\epsilon_1}\frac{\epsilon_{sfs}P}{k_{sfs}} - c_{sfs\epsilon_2}\frac{\epsilon_{sfs}^2}{k_{sfs}} + A^2(\vartheta)\frac{\partial}{\partial \xi_j}\left[\left(\nu + \frac{\nu_{sfs}}{\sigma_\epsilon}\right)\frac{\partial \epsilon_{sfs}}{\partial \xi_j}\right]. \tag{161}$$

D. Expanding grid with correction terms

In the present section, the new correction terms due to noncommutativity are accounted for, as appearing in Eqs. (120), (124), and (125). These terms are involving the derivatives of the filter width Δ. In the general case it would be necessary to use the change of variables (152) with the derivatives (153) to calculate the material derivative of Δ, so that the expression would be

$$\frac{D\Delta}{Dt} = \frac{\partial \Delta}{\partial t} + \bar{u}_k\frac{\partial \Delta}{\partial x_k} = \frac{\partial \Delta}{\partial \vartheta} + \frac{\xi_k}{A(\vartheta)}\frac{dA(\vartheta)}{d\vartheta}\frac{\partial \Delta}{\partial \xi_k} + \bar{u}_k A(\vartheta)\frac{\partial \Delta}{\partial \xi_k} = \frac{\partial \Delta}{\partial \vartheta} + A(\vartheta)\left(\bar{u}_k - V_k\right)\frac{\partial \Delta}{\partial \xi_k}. \tag{162}$$

However, in the present application, the change of variables (152) is much simpler because the filter width Δ is uniform in space and is only a function of time implying that

$$\frac{D\Delta}{Dt} = \frac{\partial \Delta}{\partial t} \equiv \frac{\partial \Delta}{\partial \vartheta}. \tag{163}$$

As a result, the continuity equation (155) remains unchanged whereas the momentum equation (157) becomes

$$\begin{aligned}\frac{\partial \bar{u}_i}{\partial \vartheta} + A(\vartheta)\frac{\partial(\bar{u}_i\bar{u}_j)}{\partial \xi_j} - V_j A(\vartheta)\frac{\partial \bar{u}_i}{\partial \xi_j} &= \frac{\partial \Delta}{\partial \vartheta}\frac{\partial \bar{u}_i}{\partial \Delta}\\ -\frac{A(\vartheta)}{\rho}\frac{\partial \bar{p}}{\partial \xi_i} + A^2(\vartheta)\nu\frac{\partial^2 \bar{u}_i}{\partial \xi_j \partial \xi_j} - A(\vartheta)\frac{\partial \tau_{ij}}{\partial \xi_j}&,\end{aligned} \tag{164}$$

with this time

$$\frac{\partial \bar{u}_j}{\partial \xi_j} + A(\vartheta)\frac{\partial \Delta}{\partial \xi_j}\frac{\partial \bar{u}_j}{\partial \Delta} = 0 \tag{165}$$

but the commutation term appearing in Eq. (165) vanishes here because of the use of a uniform grid. The subfilter turbulent energy equation (158) including the corrective terms reads

$$\begin{aligned}\frac{\partial k_{sfs}}{\partial \vartheta} + A(\vartheta)\frac{\partial}{\partial \xi_k}\left(k_{sfs}\bar{u}_k\right) - V_k A(\vartheta)\frac{\partial k_{sfs}}{\partial \xi_k} &= P + \frac{\partial \Delta}{\partial \vartheta}\frac{\partial k_{sfs}}{\partial \Delta}\\ -\epsilon_{sfs} + A^2(\vartheta)\frac{\partial}{\partial \xi_j}\left[\left(\nu + \frac{\nu_{sfs}}{\sigma_k}\right)\frac{\partial k_{sfs}}{\partial \xi_j}\right]&\end{aligned} \tag{166}$$

and the subfilter scale dissipation rate equation (161) becomes

$$\begin{aligned}\frac{\partial \epsilon_{sfs}}{\partial \vartheta} + A(\vartheta)\frac{\partial}{\partial \xi_k}\left(\epsilon_{sfs}\bar{u}_k\right) - V_k A(\vartheta)\frac{\partial \epsilon_{sfs}}{\partial \xi_k} &= c_{sfs\epsilon_1}\frac{\epsilon_{sfs}}{k_{sfs}}\left[P + \frac{\partial \Delta}{\partial \vartheta}\frac{\partial k_{sfs}}{\partial \Delta}\right]\\ -c_{sfs\epsilon_2}\frac{\epsilon_{sfs}^2}{k_{sfs}} + A^2(\vartheta)\frac{\partial}{\partial \xi_j}\left[\left(\nu + \frac{\nu_{sfs}}{\sigma_\epsilon}\right)\frac{\partial \epsilon_{sfs}}{\partial \xi_j}\right]&,\end{aligned} \tag{167}$$

with the approximations

$$\frac{\partial \bar{u}_i}{\partial \Delta} \approx \frac{\widetilde{\bar{u}}_i - \bar{u}_i}{\widetilde{\Delta} - \Delta} \tag{168}$$

and

$$\frac{\partial k_{sfs}}{\partial \Delta} \approx \frac{\widetilde{k_{sfs}} - k_{sfs}}{\widetilde{\Delta} - \Delta} \qquad \frac{\partial \epsilon_{sfs}}{\partial \Delta} \approx \frac{\widetilde{\epsilon_{sfs}} - \epsilon_{sfs}}{\widetilde{\Delta} - \Delta} \tag{169}$$

using a superfilter such that $\widetilde{\Delta} = 2\Delta$, as introduced in Sec. III E and applied on the current turbulence field.

E. Conditions of computation

In the present case, the simulations are performed on a Cartesian mesh with a grid spacing which is uniform and isotropic in the three directions of space. The computational mesh in the physical space $(\boldsymbol{x}, t)$ is not fixed but it is expanding so that the step size $\Delta_{(\Omega)}$ associated with the cell Ω is given by $\Delta_{(\Omega)} = (\delta x_{1(\Omega)} \delta x_{2(\Omega)} \delta x_{3(\Omega)})^{1/3}$ increases in time in order to account for the increase of turbulence scales during decay. The grid size $\Xi_{(\Omega)}$ in the transformed space $(\boldsymbol{\xi}, \vartheta)$ is constant in space and time and is computed as $\Xi_{(\Omega)} = (\delta \xi_{1(\Omega)} \delta \xi_{2(\Omega)} \delta \xi_{3(\Omega)})^{1/3}$ so that

$$\Xi_{(\Omega)} = A(\vartheta) \Delta_{(\Omega)}(\vartheta), \tag{170}$$

in which $\Xi_{(\Omega)}$ is constant while $\Delta_{(\Omega)}$ increases in time. Obviously

$$\frac{\partial \Xi_{(\Omega)}}{\partial \vartheta} = 0 \quad \text{and} \quad \frac{\partial \Xi_{(\Omega)}}{\partial \xi_k} = 0 \tag{171}$$

but

$$\frac{\partial \Delta_{(\Omega)}}{\partial \vartheta} = \frac{\partial}{\partial \vartheta} \left(\frac{\Xi_{(\Omega)}}{A(\vartheta)} \right) = -\frac{dA(\vartheta)}{A^2(\vartheta) d\vartheta} \Xi_{(\Omega)} \quad \text{and} \quad \frac{\partial \Delta_{(\Omega)}}{\partial \xi_k} = 0. \tag{172}$$

The variable change allows to consider a constant grid size $\Xi_{(\Omega)}$ in a transformed variable coordinate system $(\boldsymbol{\xi}, \vartheta)$ in place of a variable grid size $\Delta_{(\Omega)}(\vartheta)$ in a constant coordinate system $(\boldsymbol{x}, t)$ as illustrated in Figure 1. Solving Eqs. (145) and (146) leads to the evolution of the turbulent energy given by

$$k(t) = k_0 \left(1 + \frac{\epsilon_0 t}{n k_0} \right)^{-n} \tag{173}$$

and the dissipation-rate

$$\epsilon(t) = \epsilon_0 \left(1 + \frac{\epsilon_0 t}{n k_0} \right)^{-(n+1)}, \tag{174}$$

where according to Eq. (144)

$$n = \frac{1}{c_{\epsilon_2} - 1} = \frac{2m+2}{m+3}, \tag{175}$$

and where k_0 and ϵ_0 denote the turbulent energy and the dissipation-rate at the initial time, respectively. Considering that the dissipation process of the small scales by the molecular viscosity implies a global increase of the characteristic turbulence scales in time, it is desirable to increase the step size accordingly. From Eqs. (173) and (174), one can recover the characteristic scale $\mathcal{L}$ evolution law

$$\mathcal{L}(t) = \frac{k^{3/2}(t)}{\epsilon(t)} = \mathcal{L}_0 \left(1 + \frac{\epsilon_0 t}{n k_0} \right)^{1-n/2}, \tag{176}$$

where $\mathcal{L}_0 = k_0^{3/2}/\epsilon_0$ is the characteristic scale at the initial time. Consequently, with the aim to conform to the decaying spectrum evolution during the computation, we simply suggest to use the

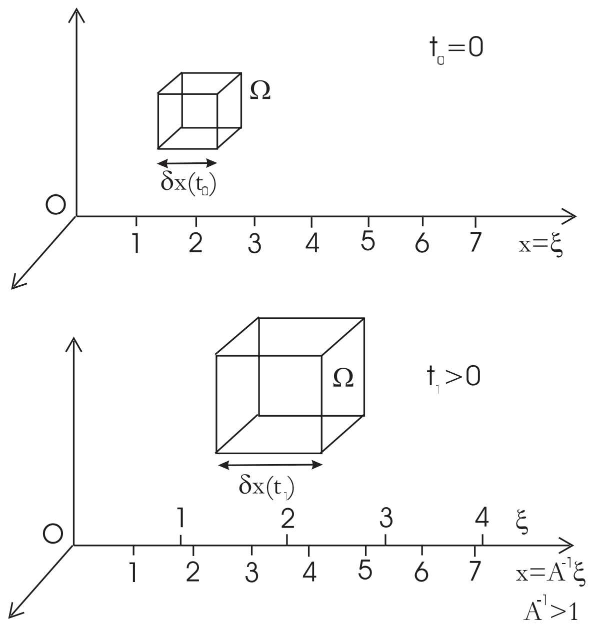

FIG. 1. Sketch of the expanding discretization grid and attached coordinate system (the numerical values are arbitrary).

function $A(t)$ in the form

$$A(t) = (1 + \alpha t)^{-p} \tag{177}$$

in which α and p are numerical constants chosen to approximately reproduce the scale evolution of the turbulence field, implying that

$$\frac{1}{A(t)}\frac{dA(t)}{dt} = -\frac{\alpha p}{1 + \alpha t}. \tag{178}$$

For $t = 0$, at the initial state, $A(t = 0) = 1$, so that $\Delta_{(\Omega)}(\vartheta = 0) = \Xi_{(\Omega)}$.

As a result of interest, one can remark that during the decay, as $t = \vartheta$, $0 < A(\vartheta) < 1$, and $dA/d\vartheta(\vartheta) < 0$ so that the sign of $V_i(\boldsymbol{\xi}, \vartheta)$ appearing in the most general transport equations (164), (166), and (167) is the same as the one of $x_{i(\Omega)}$, and can be physically interpreted as the expansion velocity in physical space of the computational grid as indicated by Eq. (156). We note also that $V_i(\boldsymbol{\xi}, \vartheta)$ is not divergence free. From Eqs. (156) and (172), one finds indeed

$$div_{\xi}(\boldsymbol{V}) = \frac{\partial V_j(\boldsymbol{\xi}, \vartheta)}{\partial \xi_j} = -\frac{3}{A^2(\vartheta)}\frac{dA(\vartheta)}{d\vartheta} = \frac{3}{\Xi_{(\Omega)}}\frac{d\Delta_{(\Omega)}(\vartheta)}{d\vartheta}. \tag{179}$$

The numerical discretization of the above equations is made in the $(\boldsymbol{\xi}, \vartheta)$ space-time as specified in the Secs. VI C and VI D. During the numerical simulation the value of $A(\vartheta) = (1 + \alpha\vartheta)^{-p}$ is obtained directly from Eq. (177) while the material derivative is simply given by

$$\frac{D\Delta_{(\Omega)}}{Dt} \equiv \frac{d\Delta_{(\Omega)}}{d\vartheta} = \alpha p(1 + \alpha\vartheta)^{p-1}\,\Xi_{(\Omega)}. \tag{180}$$

(We recall that $\vartheta \equiv t$ for functions of a single variable.) From Eq. (176), we get

$$\frac{\mathcal{L}}{\mathcal{L}_0} = \left(1 + \frac{\epsilon_0\vartheta}{nk_0}\right)^{1-n/2}. \tag{181}$$

Comparing with the equation for the grid step evolution,

$$\frac{\Delta_{(\Omega)}(\vartheta)}{\Delta_{(\Omega)}(0)} = \frac{A(0)}{A(\vartheta)} = (1 + \alpha\vartheta)^p, \tag{182}$$

one gets the value for the numerical constants

$$p = \frac{2-n}{2} = \frac{2}{m+3} \quad \text{and} \quad \alpha = \frac{\epsilon_0}{nk_0} = \left(\frac{m+3}{2m+2}\right)\frac{\epsilon_0}{k_0}. \tag{183}$$

F. Finite volume method

The numerical code[47,48] used for the simulations of the decaying turbulence is based on the finite volume technique. In this section, we briefly show that the transformed transport equations (164), (166), and (167) can be rewritten in a similar form as for fixed grid but considering however the relative velocity computed as the difference between the filtered flow velocity and the mesh velocity defined in Eq. (156). Let us consider Eq. (164). The first step consists in multiplying this equation by $A^{-3}(\vartheta)$, and to rearrange the terms appearing in the left hand-side in the following way:

$$A^{-3}\frac{\partial \bar{u}_i}{\partial \vartheta} = \frac{\partial}{\partial \vartheta}(A^{-3}\bar{u}_i) - \bar{u}_i\frac{\partial}{\partial \vartheta}(A^{-3}) = \frac{\partial}{\partial \vartheta}(A^{-3}\bar{u}_i) + 3\bar{u}_i A^{-4}\frac{\partial A}{\partial \vartheta}, \tag{184}$$

$$A^{-2}\frac{\partial}{\partial \xi_j}(\bar{u}_i\bar{u}_j) = \frac{\partial}{\partial \xi_j}(A^{-2}\bar{u}_i\bar{u}_j) - \bar{u}_i\bar{u}_j\frac{\partial}{\partial \xi_j}(A^{-2}), \tag{185}$$

$$-A^{-2}V_j\frac{\partial \bar{u}_i}{\partial \xi_j} = -\frac{\partial}{\partial \xi_j}(A^{-2}V_j\bar{u}_i) + A^{-2}\bar{u}_i\frac{\partial V_j}{\partial \xi_j} = -\frac{\partial}{\partial \xi_j}(A^{-2}V_j\bar{u}_i) + 3\bar{u}_i A^{-4}\frac{\partial A}{\partial \vartheta}. \tag{186}$$

Using Eqs. (184), (185), and (186), as well as Eq. (170) for the filter width $\Delta_{(\Omega)}(\vartheta)$, Eq. (164) then becomes

$$\frac{\partial}{\partial \vartheta}\left(\Delta^3_{(\Omega)}\bar{u}_i\right) + A(\vartheta)\Delta^3_{(\Omega)}\frac{\partial}{\partial \xi_j}\left((\bar{u}_j - V_j)\bar{u}_i\right) = \Delta^3_{(\Omega)}\frac{\partial \Delta}{\partial \vartheta}\frac{\partial \bar{u}_i}{\partial \Delta}$$
$$+\Delta^3_{(\Omega)}\left(-\frac{A(\vartheta)}{\rho}\frac{\partial \bar{p}}{\partial \xi_i} + A^2(\vartheta)\nu\frac{\partial^2 \bar{u}_i}{\partial \xi_j\partial \xi_j} - A(\vartheta)\frac{\partial \tau_{ij}}{\partial \xi_j}\right) \tag{187}$$

or equivalently,

$$\frac{\delta}{\delta t}\left(\Delta^3_{(\Omega)}\bar{u}_i\right) + \Delta^3_{(\Omega)}\frac{\delta}{\delta x_j}\left((\bar{u}_j - V_j)\bar{u}_i\right) = \Delta^3_{(\Omega)}\frac{\delta \Delta}{\delta t}\frac{\delta \bar{u}_i}{\delta \Delta}$$
$$+\Delta^3_{(\Omega)}\left(-\frac{1}{\rho}\frac{\delta \bar{p}}{\delta x_i} + \nu\frac{\partial^2 \bar{u}_i}{\partial x_j\partial x_j} - \frac{\partial \tau_{ij}}{\partial x_j}\right). \tag{188}$$

After integration on the control volume $\Delta^3_{(\Omega)}$, one finally gets the discretized equation written in term of finite volume

$$\frac{\delta}{\delta t}\left(\Delta^3_{(\Omega)}\bar{u}_{i_{(\Omega)}}\right) + \sum_{\sigma_{(\Omega)}}\left[\bar{u}_i(\bar{u}_j - V_j)n_j + \bar{p}n_i\right]S_\sigma = \sum_{\sigma_{(\Omega)}}(2\nu S_{ij} - \tau_{ij})n_jS_\sigma$$
$$+\Delta^3_{(\Omega)}\frac{\delta \Delta_{(\Omega)}}{\delta t}\frac{\delta \bar{u}_{i_{(\Omega)}}}{\delta \Delta_{(\Omega)}}, \tag{189}$$

where $\bar{u}_{i_{(\Omega)}}$ is the mean averaged velocity on the cell, $\boldsymbol{n}$ is the unit vector normal to the surface S_σ surrounding the cell Ω and S_{ij} denotes the strain rate tensor. This resulting equation written on moving grids is of the Arbitrary Eulerian Lagrangian (ALE) formulation.[52,53] As expected, the velocity vector in the convective term is the relative velocity $\boldsymbol{u} - \boldsymbol{V}$. The transport equations (166) and (167) are treated in the same way leading to the corresponding discretized equations obtained with the finite volume technique as follows:

$$\frac{\delta}{\delta t}\left(\Delta^3_{(\Omega)}k_{sfs_{(\Omega)}}\right) + \sum_{\sigma_{(\Omega)}}\left[k_{sfs}(\bar{u}_j - V_j)n_j\right]S_\sigma = \sum_{\sigma_{(\Omega)}} j_{k_j}n_jS_\sigma$$
$$+\Delta^3_{(\Omega)}\left(P + \frac{\delta \Delta_{(\Omega)}}{\delta t}\frac{\delta k_{sfs_{(\Omega)}}}{\delta \Delta_{(\Omega)}} - \epsilon_{sfs_{(\Omega)}}\right) \tag{190}$$

and

$$\frac{\delta}{\delta t}\left(\Delta^3_{(\Omega)}\epsilon_{sfs_{(\Omega)}}\right) + \sum_{\sigma(\Omega)}\left[\epsilon_{sfs}(\bar{u}_j - V_j)n_j\right]S_\sigma = \sum_{\sigma(\Omega)} j_{\epsilon_j} n_j S_\sigma$$

$$+\Delta^3_{(\Omega)}\left[c_{sfs\epsilon_1}\frac{\epsilon_{sfs_{(\Omega)}}}{k_{sfs_{(\Omega)}}}\left(P + \frac{\delta\Delta_{(\Omega)}}{\delta t}\frac{\delta k_{sfs_{(\Omega)}}}{\delta\Delta_{(\Omega)}}\right) - c_{sfs\epsilon_2}\frac{\epsilon^2_{sfs_{(\Omega)}}}{k_{sfs_{(\Omega)}}}\right], \quad (191)$$

where j_{k_j} and j_{ϵ_j} are related to the turbulent diffusion processes.

G. Numerical results

Figure 2 displays the decay of the three-dimensional spectra starting from the initial time for the PITM simulations performed both on the fixed and moving meshes at different time advancements, denoted PITM1 and PITM2, respectively. The simulation performed on the moving mesh (PITM2) consists in solving the filtered transport equations written in the ALE formulation including here the commutation terms (equations of Sec. VI D). As an expected result, one can see that all simulations are able to reproduce the evolutions of the spectrum at different times in accordance with the Kolmogorov law. One can see that the inertial transfer zone for the energy cascade computed initially at the chosen Reynolds number $Re \approx 5000$ is well visible. As expected also, the PITM2 performed on the moving mesh allows a better description of the energetic region of the spectrum than the PITM1 simulation, especially in the productive zone at low wave numbers. This is because of the dynamic conforming of the discretization points to the varying spectrum. In particular, the distribution of the turbulent energy associated with the PITM2 is more accurately described in the lower κ wave numbers region because of the increase of the turbulence length-scale which evolves in time according to the law given by Eq. (181). The maxima of the spectrum $E(\kappa)$ as well as the differences $E(\kappa_2) - E(\kappa_1)$ for the PITM2 and PITM1 simulations are listed in Table I at different times $t = t_1, t_2, t_3$. The index 2 pertains to the moving mesh simulation while index 1 pertains to the fixed mesh simulation. As a result, one can see that the difference of the maximum of the spectrum $\delta E = E(\kappa_2) - E(\kappa_1)$ between the case with coarsened grid and fixed grid increases whereas the

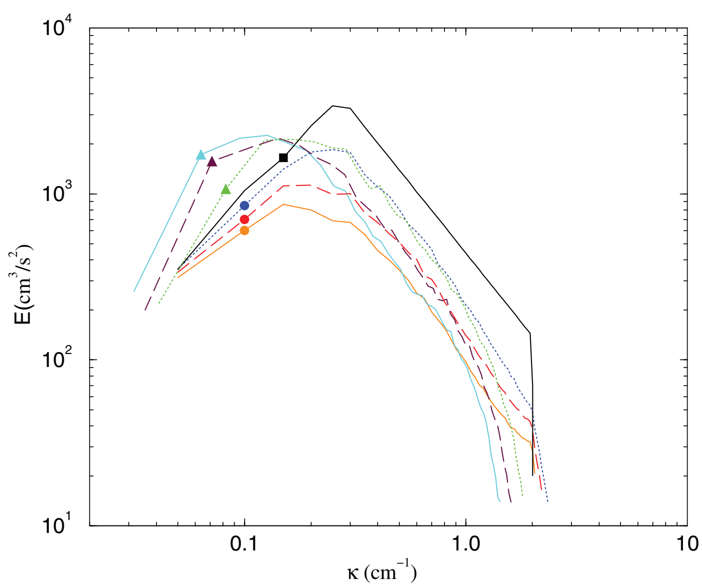

FIG. 2. PITM simulations of the homogeneous decay of the energy spectra at different time advancement $t = t_1, t_2, t_3$ performed on fixed and moving meshes ($\kappa_c = 2\,\text{cm}^{-1}$). Initial spectrum given by Eq. (139): —■—. PITM1 (fixed mesh): t_1: blue, . . . ● . . . , t_2: red, – – ● – – , and t_3: orange, —●—. PITM2 (moving mesh, equations with commutation terms): t_1: green, · · · ▲ · · · , t_2: maroon, – – ▲ – – , and t_3: cyan, — ▲ —.

TABLE I. Maximum of the spectrum at different time advancement for the PITM simulations performed on the fixed and moving meshes including the computation of the commutation terms.

	$E(\kappa_2)\,(\mathrm{cm}^3/\mathrm{s}^2)$	$E(\kappa_1)$	$\kappa_2\,(\mathrm{cm}^{-1})$	κ_1	$\delta E\,(\mathrm{cm}^3/\mathrm{s}^2)$	$\delta\kappa\,(\mathrm{cm}^{-1})$
t_1	2131	1849	0.164	0.250	282	−0.0861
t_2	2161	1002	0.140	0.200	1159	−0.0600
t_3	2245	863	0.127	0.150	1382	−0.0231

difference of the wave numbers $\delta\kappa = \kappa_2 - \kappa_1$ decreases. These results concerning the evolution of the spectra $E(\kappa_2)$ and $E(\kappa_1)$ can be explained if one considers that the large scale energy decreases more slowly than the small scale energy and indeed, the larger the eddies, the longer is their time scale. Big eddies are more permanent and this is recovered in the moving mesh calculation which is conforming to spectrum evolution. On the contrary, in the fixed grid calculation, the big eddies are decaying too much because the calculation box becomes too small, and this is rather unphysical. In complement to Figure 2, the new Figure 3 now displays the decay of the three-dimensional spectra, for both PITM simulations performed on the moving meshes but with and without the commutation terms appearing in the LES equations, denoted PITM2 (equations of Sec. VI D) and PITM3 (equations of Sec. VI C), respectively. When comparing globally the results between these two simulations, one can see that the curves associated with the PITM2 present a more regular evolution than the one associated with the PITM3, especially at low wave number. At high wave numbers, the curves associated with the PITM2 and PITM3 present subtle differences. Indeed, the PITM2 curves are slightly more dissipative than the PITM3 curves which are located slightly above the corresponding PITM2 spectrum. Reasoning on the turbulence kinetic energy, this can be explained physically by the fact that for the PITM3, the term

$$\int_0^t E(\kappa_c)\frac{\partial \kappa_c}{\partial t}dt, \tag{192}$$

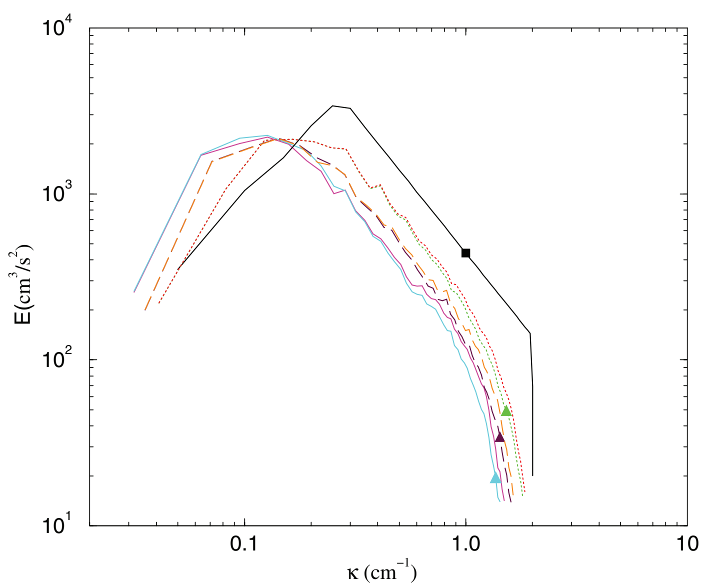

FIG. 3. PITM simulations of the homogeneous decay of the energy spectra at different time advancement $t = t_1$, t_2, t_3 performed on the moving mesh ($\kappa_c = 2\,\mathrm{cm}^{-1}$). Initial spectrum given by Eq. (139): —■—. PITM2 (equations with commutation terms): t_1: green, $\cdots$ ▲ $\cdots$, t_2: maroon, $--$ ▲ $--$, and t_3: cyan, — ▲ —. PITM3 (equations without commutation terms): t_1: red, $\cdots$, t_2: orange, $--$, and t_3: violet, —.

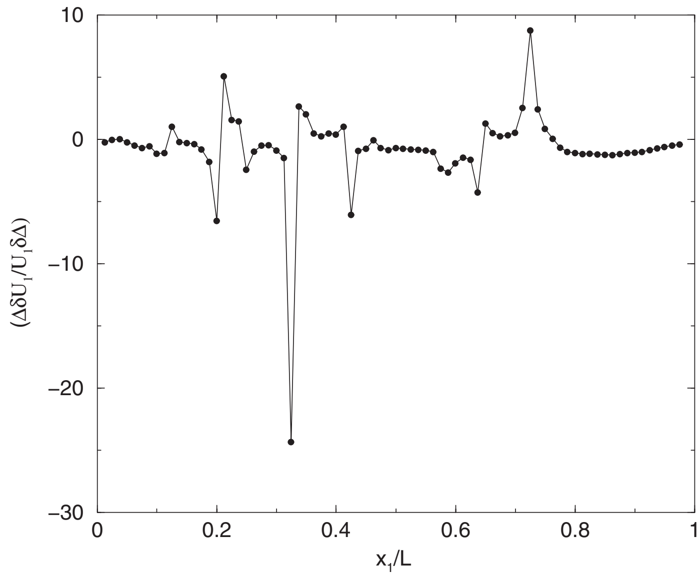

FIG. 4. Computation of the instantaneous dimensionless commutation term at a given time $(\Delta\delta\bar{u}_i)/(\bar{u}_i\delta\Delta)$ versus the dimensionless distance x_1/L.

with

$$\frac{\partial \kappa_c}{\partial t} < 0 \tag{193}$$

appearing in Eq. (58) in its instantaneous form is neglected. It means that this part of energy due to the variation of cutoff is not allowed to cross the cutoff as it should, creating an energy accumulation in the box. As this equation shows, the effect would be more important on coarse grids because the cutoff would occur earlier in the spectrum. With the aim to get an additional insight of the effect of the commutation terms on the equations, Figure 4 plots the instantaneous evolution of the dimensionless commutation term $(\Delta\delta\bar{u}_i)/(\bar{u}_i\delta\Delta)$ at a given time versus the dimensionless distance x_1/L. Although the averaging of the commutation term in the homogeneous direction reduces to zero in absence of mean convective velocity, one can see that the signal is characterized by appreciable fluctuations in space that should therefore acting on the instantaneous filtered LES equations. So, commutation introduces both global effects on energy levels and local effects in fluctuating terms. Figure 5 shows the time decay of the turbulence, respectively, for the subfilter energy $\langle k_{sfs}\rangle$, the resolved scale energy $<k_{les}>$, and the total energy for the PITM2 and PITM3 simulations performed on the moving mesh. The decay laws shown for both simulations look very similar but it is important to notice that the total and large scale energies for the PITM3 simulation decreases at a slightly lower rate than for the PITM2 simulation. From a physical point of view, this result fully confirms the observation and discussion made for Figure 3 showing that the level of energy in the density spectrum at higher wave numbers is slightly but undoubtedly larger for the PITM2 calculation than for the PITM3 calculation. Even if these observations involve small amounts of energy, they clearly show some aspects of the role of commutation terms and how to account for them. Moreover, one can remark also that the effect observed here is cumulative and increases with time. The decay law given by Eq. (173) where k is in the present case obtained as the sum of the subfilter and resolved parts of energy leads to the slope close to $n = 1.1$ according to the usual value of the coefficient $c_{\epsilon_2} \approx 1.9$ for $m = 1.4$. More investigations on the PITM results can be pursued but this first analysis conducted here is however sufficient to determine the role of the filtering in the LES equations, even if the influence of the commutation terms finally appears not crucial in the present test case. The reason is certainly due to the slow decay in time of the filter width which is not sufficient to induce strong commutation errors. As mentioned earlier, the grid of the mesh has been coarsened according to the given law (176) that expresses the increase of the turbulence macroscale during decay governed by the Kolmogorov

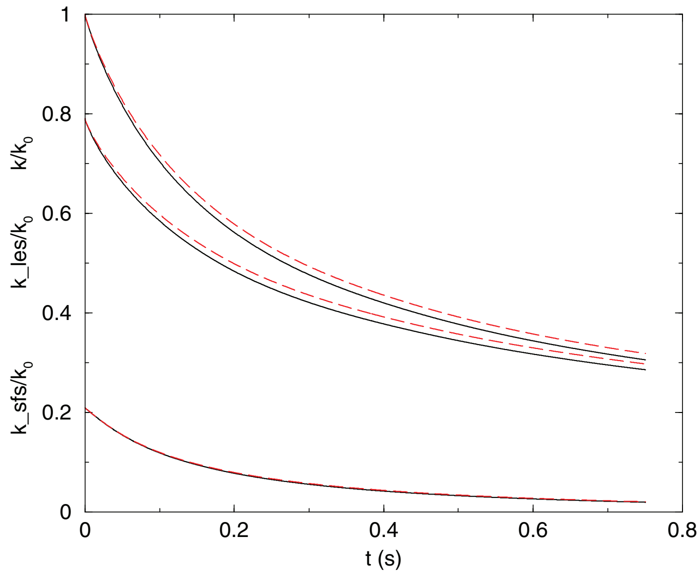

FIG. 5. Homogeneous decay of the turbulent kinetic energy k/k_0, the resolved turbulent energy k_{les}/k_0, and the subfilter turbulent energy k_{sfs}/k_0 with respect to the time advancement performed on the moving mesh ($\kappa_c = 2\,\mathrm{cm}^{-1}$); equations with commutation terms : ——; equations without commutation terms : red, - - - -.

cascade. This numerical procedure optimizes the mesh resolution and grid size because at each time advancement, the grid evolution conforms to the energy spectrum changes and thus remains always adapted for solving the filtered Navier-Stokes equations including also the transport equations for the turbulent energy and the dissipation rate. But in an attempt to investigate the commutation effects in a less favorable case, it is also worth performing PITM simulations on a moving mesh where the grid expands more rapidly, for instance twice faster than the normal expansion rate. Of course, this later case is more relevant for a purely numerical test than for a physical analysis. Indeed, it is obviously less appropriate to account for the dynamics of turbulence decay. The value of p given in Eq. (182) was $p = 2/(m + 3) = 0.45455$ for $m = 1.4$ when we performed the PITM2 and PITM3 calculations and we now propose to test to use twice this value, just to check how the method works. Figure 6 displays the decay of the three-dimensional energy spectrum for the PITM4 and PITM5 simulations performed on the new moving mesh, respectively, with and without solving the commutation terms. As expected, the PITM4 curves are more dissipative than the PITM5 curves in the high wave number range. At high wave numbers, one can see that the energy spectrum associated with the PITM5 (without the commutation terms) is slightly higher than the one associated with the PITM4 (with the commutation terms). As mentioned in Sec. III B concerning the statistical interpretation in the spatial and spectral spaces, this outcome means that a part of energy contained into the resolved scales is transferred into the modeled spectral zone. Globally, the results still remain acceptable for both PITM simulations because the $\kappa^{-5/3}$ Kolmogorov law is still well verified during the decay of the turbulent energy, although the filter width now becomes too large to account for the intermediate scales of the flow that should be computed by the numerical scheme instead of being here modeled. Indeed, physically, the increase in time of the grid size during decay implies that the relative part of modeled energy gradually increases, to the detriment of the resolved part of energy, because the cutoff wave number κ_c gets smaller. In Figure 6, it is clear that the spectrum falloff happens earlier than on the spectrum shown in Figure 2 or 3. This result is in perfect agreement with the theory prediction because the time derivative of the cutoff wave number $E(\kappa_c)\partial\kappa_c/\partial t$ is now stronger in its absolute value and hence, the commutation errors are higher. One cannot miss to remark however that the energy spectrum densities shown in Figure 6 extend further into the smaller wave number range. Although this drawback is not the purpose of the present work (because it is not really relevant to the κ_c commutation problem), we shall try to propose an explanation. This behavior seems unexpected because the grid is expanding more rapidly. The calculation box in the

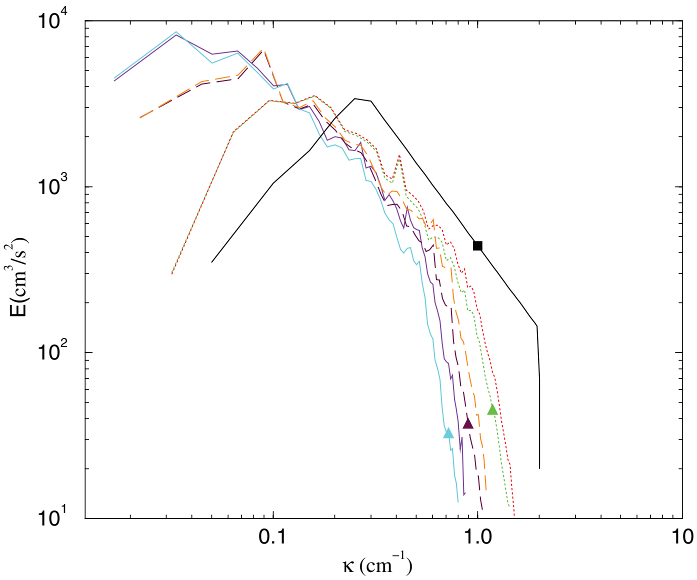

FIG. 6. PITM simulations of the homogeneous decay of the energy spectra at different time advancement $t = t_1$, t_2, t_3 performed on the moving mesh where the grid expands twice faster the normal expansion rate ($\kappa_c = 2\,\mathrm{cm}^{-1}$). Initial spectrum given by Eq. (139): —■—. PITM4 (equations with commutation terms): t_1: green, ··· ▲ ···, t_2: maroon, – – ▲ – –, and t_3: cyan, — ▲ —. PITM5 (equations without commutation terms): t_1: red, ···, t_2: orange, – –, and t_3: violet, —.

physical space is larger, the corresponding spectral box is correlatively smaller, and thus the large eddies should be well resolved anyway. But, considering that the large eddies tend to occupy all the space offered to them, energy can reach lower wave numbers in a slow process however. Probably this process is shunted by the fact that periodic boundary conditions are still applied in the same way when expanding grids are used, thus introducing artificial very big eddies. Let us mention again that the PITM4 and PITM5 cases are to be understood as technical tests that remain purposely far from the best physical choices.

VII. CONCLUSION

In this work, we have focused on the extension of the PITM method to the case of variable filter width either in time or in space. The complex expressions of the commutation terms appearing in the filtered turbulence equations have been analytically derived using the rules of convolution operators with variable kernels associated with a comprehensive mathematical formalism. Then, the general formalism has been applied to the particular case of the PITM method. Even if the proposed technique can be applied to all commutation terms appearing in the transport equations of the turbulence field, the emphasis has been laid upon the commutation effect in the material derivative which was expected to be of a primary importance. From a physical point of view, we have shown that the commutation term can be interpreted as an energy exchange from the resolved scales to the modeled scales and vice-versa. The technique is intended to applications to turbulent flow simulations with strongly variable meshes in time or space. The estimate for the noncommutation terms makes use of a superfilter superimposed to the simulation filter. With the aim to illustrate the filtering process in LES, the application to the decay of homogeneous turbulence has been considered. As a result of interest, it appears that the PITM2 simulation solving the filtered equations written in the ALE formulation including the commutation terms is able to accurately reproduce the decay of the spectrum, in the region of the large wave numbers implying the $\kappa^{-5/3}$ Kolmogorov decay but also in the region of slow wave numbers dominated by large carrying scales of energy. In this particular case, it has been shown that the accounting for the commutation terms in the filtered LES equations improves the solution even if their influence on the equations is not crucial here, because of the slow decay in time of the filter width. For the moving mesh where the grid expands faster than the normal expansion rate, even when the commutation errors are higher, we have shown that the present method still continues to work correctly. This conclusion however pertains only to a particular flow which remains close to spectral equilibrium during the time.

APPENDIX: MATHEMATICS IN PHYSICAL AND SPECTRAL SPACES

1. Cutoff filter in the spectral and physical spaces

The spectral cutoff filter is defined from

$$\widehat{G}(\boldsymbol{\kappa}) = H(\boldsymbol{\kappa_c} - \boldsymbol{\kappa}), \tag{A1}$$

where H denotes the Heaviside distribution and $\boldsymbol{\kappa_c}$ is the cutoff wave-number. Applying the inverse Fourier transform of the filter function $\widehat{G}$ leads to

$$G(\boldsymbol{x}) = \frac{1}{(2\pi)^3} \int H(\boldsymbol{\kappa_c} - \boldsymbol{\kappa}) e^{i\boldsymbol{\kappa}\boldsymbol{x}} d\boldsymbol{\kappa}. \tag{A2}$$

If one denotes

$$\mathcal{M}(f) = \oiint_{S(\kappa)} f(\boldsymbol{\kappa})\, dA(\kappa) \tag{A3}$$

as the spherical mean of the function f, then it is possible to write

$$G(\boldsymbol{x}) = \frac{1}{(2\pi)^3} \int_0^{\kappa_c} \mathcal{M}\left(e^{i\boldsymbol{\kappa}\boldsymbol{x}}\right) d\kappa. \tag{A4}$$

If working in spherical coordinates, $\kappa_1 = \kappa \sin\theta \cos\phi$, $\kappa_2 = \kappa \sin\theta \sin\phi$, and $\kappa_3 = \kappa \cos\theta$, the spherical mean of the function $e^{i\kappa z}$ can be easily calculated from

$$\mathcal{M}\left(e^{i\boldsymbol{\kappa}\boldsymbol{x}}\right) = \int_0^{\pi} \int_0^{2\pi} \kappa^2 \sin\theta\, e^{i\kappa x \cos\theta} d\theta d\phi. \tag{A5}$$

Then, using the variable change

$$\begin{cases} u = \cos\theta \\ du = -\sin\theta d\theta \end{cases}, \tag{A6}$$

one get

$$\mathcal{M}\left(e^{i\boldsymbol{\kappa}\boldsymbol{x}}\right) = \int_{-1}^{+1} 2\pi\kappa^2 e^{i\kappa x u} du = 2\pi\kappa^2 \left[\frac{e^{i\kappa x u}}{i\kappa x}\right]_{-1}^{+1} = \frac{4\pi\kappa}{x} \sin\kappa x, \tag{A7}$$

so that the final result is

$$G(\boldsymbol{x}) = \frac{1}{(2\pi)^3} \int_0^{\kappa_c} \frac{4\pi\kappa}{x} \sin\kappa z\ d\kappa \tag{A8}$$

or equivalently,

$$G(\boldsymbol{x}) = \frac{4\pi}{(2\pi x)^3} \left[\sin(\kappa_c x) - \kappa_c x \cos(\kappa_c x)\right]. \tag{A9}$$

2. Variable convolution kernels

Considering the filtered value of a turbulent field quantity $f(\boldsymbol{x})$, if the flow is homogeneous, a constant convolution kernel G can be used such that

$$\overline{\phi}(\boldsymbol{x}) = \int_{\mathbb{R}^3} G(\boldsymbol{x} - \boldsymbol{\xi}) \phi(\boldsymbol{\xi}) d\boldsymbol{\xi} = (G * \phi)(\boldsymbol{x}), \tag{A10}$$

with the normalization condition

$$\int_{\mathbb{R}^3} G(\boldsymbol{\xi}) d\boldsymbol{\xi} = 1. \tag{A11}$$

Note that this formula is mathematically equivalent to

$$\overline{\phi}(\boldsymbol{x}) = \int_{\mathbb{R}^3} G(\boldsymbol{\xi})\phi(\boldsymbol{x}-\boldsymbol{\xi})d\boldsymbol{\xi} = (G * \phi)(\boldsymbol{x}) \tag{A12}$$

implying that

$$\frac{\partial\overline{\phi}(\boldsymbol{x})}{\partial x_i} = \int_{\mathbb{R}^3} G(\boldsymbol{\xi})\frac{\partial\phi}{\partial x_i}(\boldsymbol{x}-\boldsymbol{\xi})d\boldsymbol{\xi} \tag{A13}$$

or in shorthand notation

$$\frac{\partial\overline{\phi}(\boldsymbol{x})}{\partial x_i} = \left(G * \frac{\partial\phi}{\partial x_i}\right)(\boldsymbol{x}), \tag{A14}$$

so that

$$\frac{\partial\overline{\phi}}{\partial x_i}(\boldsymbol{x}) = \overline{\frac{\partial\phi}{\partial x_i}}(\boldsymbol{x}). \tag{A15}$$

Incidentally, one remarks also that

$$\frac{\partial\overline{\phi}(\boldsymbol{x})}{\partial x_i} = \left(\frac{\partial G}{\partial x_i} * \phi\right)(\boldsymbol{x}). \tag{A16}$$

These previous relations no longer hold when the filter size varies in time or/and in space. In this case, the convolution kernel G is also a function of an additional parameter such as for instance the width Δ of the bell shaped curve of the filter. The filtered value is then defined from

$$\overline{\phi}(\boldsymbol{x}, t, \Delta) = \int_{\mathbb{R}^3} G(\boldsymbol{x}-\boldsymbol{\xi}, \Delta)\phi(\boldsymbol{\xi}, t)d\boldsymbol{\xi} = (G_\Delta * \phi)(\boldsymbol{x}, t) \tag{A17}$$

or equivalently,

$$\overline{\phi}(\boldsymbol{x}, t, \Delta) = \int_{\mathbb{R}^3} G(\boldsymbol{\xi}, \Delta)\phi(\boldsymbol{x}-\boldsymbol{\xi}, t)d\boldsymbol{\xi} = (G_\Delta * \phi)(\boldsymbol{x}, t). \tag{A18}$$

If the parameter Δ is attached to the space field location $\boldsymbol{x}$ and possibly variable in time t, then

$$\frac{\partial\overline{\phi}}{\partial x_i}(\boldsymbol{x}, t, \Delta) \neq \overline{\frac{\partial\phi}{\partial x_i}}(\boldsymbol{x}, t, \Delta) \tag{A19}$$

and an extra term appears in the derivatives. More precisely, taking the derivative of Eq. (A18) leads to

$$\frac{\partial\overline{\phi}(\boldsymbol{x}, t, \Delta)}{\partial x_i} = \int_{\mathbb{R}^3} \frac{\partial\Delta}{\partial x_i}\frac{\partial G(\boldsymbol{\xi}, \Delta)}{\partial\Delta}\phi(\boldsymbol{x}-\boldsymbol{\xi}, t)d\boldsymbol{\xi} + \int_{\mathbb{R}^3} G(\boldsymbol{\xi}, \Delta)\frac{\partial\phi(\boldsymbol{x}-\boldsymbol{\xi}, t)}{\partial x_i}d\boldsymbol{\xi} \tag{A20}$$

or in shorthand notation

$$\frac{\partial\overline{\phi}(\boldsymbol{x}, t, \Delta)}{\partial x_i} = \frac{\partial\Delta}{\partial x_i}\frac{\partial}{\partial\Delta}(G_\Delta * \phi)(\boldsymbol{x}, t, \Delta) + (G_\Delta * \frac{\partial\phi}{\partial x_i})(\boldsymbol{x}, t, \Delta), \tag{A21}$$

and finally

$$\frac{\partial\overline{\phi}(\boldsymbol{x}, t, \Delta)}{\partial x_i} = \frac{\partial\Delta}{\partial x_i}\frac{\partial}{\partial\Delta}\overline{\phi}(\boldsymbol{x}, t, \Delta) + \overline{\frac{\partial\phi}{\partial x_i}}(\boldsymbol{x}, t, \Delta). \tag{A22}$$

Similarly, one gets for the time derivatives

$$\frac{\partial\overline{\phi}(\boldsymbol{x}, t, \Delta)}{\partial t} = \frac{\partial\Delta}{\partial t}\frac{\partial}{\partial\Delta}\overline{\phi}(\boldsymbol{x}, t, \Delta) + \overline{\frac{\partial\phi}{\partial t}}(\boldsymbol{x}, t, \Delta). \tag{A23}$$

3. Commutation term for the cutoff filter

In the case of the spectral splitting, the commutation term $\beta_T(\phi)$ can be expressed analytically (see Sec. 8.3 on p. 437 of Ref. 20). For each variable ϕ, the Fourier transform and reverse Fourier transform are defined by

$$\phi(\boldsymbol{x}, t) = \int_{\mathbb{R}^3} \widehat{\phi}(\boldsymbol{\kappa}, t) e^{i\boldsymbol{\kappa x}} d\boldsymbol{\kappa} \tag{A24}$$

and

$$\widehat{\phi}(\boldsymbol{\kappa}, t) = \int_{\mathbb{R}^3} \phi(\boldsymbol{x}, t) e^{-i\boldsymbol{\kappa x}} d\boldsymbol{x}. \tag{A25}$$

The filtering in spectral space implies multiplication by the filter function in wave number:

$$\widehat{\bar{\phi}}(\boldsymbol{\kappa}, t) = \hat{G}_{\kappa_c}(\boldsymbol{\kappa}, t)\, \hat{\phi}(\boldsymbol{\kappa}, t). \tag{A26}$$

Applying the definition (A24) to the filtered variable $\bar{\phi}$ using the relation (A26) leads to

$$\bar{\phi}(\boldsymbol{x}, t) = \int_{\mathbb{R}^3} \widehat{\bar{\phi}}(\boldsymbol{\kappa}, t) e^{i\boldsymbol{\kappa x}} d\boldsymbol{\kappa} = \int_{\mathbb{R}^3} \hat{G}_{\kappa_c}(\boldsymbol{\kappa}, t)\, \hat{\phi}(\boldsymbol{\kappa}, t) e^{i\boldsymbol{\kappa x}} d\boldsymbol{\kappa} \tag{A27}$$

and the derivative of Eq. (A27) takes the form as

$$\frac{d\bar{\phi}(\boldsymbol{x}, t)}{dt} = \int_{\mathbb{R}^3} \left(\hat{G}_{\kappa_c}(\boldsymbol{\kappa}, t)\, \frac{d\hat{\phi}}{dt}(\boldsymbol{\kappa}, t) + \hat{\phi}(\boldsymbol{\kappa}, t) \frac{d\hat{G}_{\kappa_c}(\boldsymbol{\kappa}, t)}{dt} \right) e^{i\boldsymbol{\kappa x}} d\boldsymbol{\kappa}. \tag{A28}$$

The integration of the first term appearing in the right hand side is simply the mean variable if referring to Eq. (A27), so that Eq. (A28) can be rewritten into the following form as

$$\frac{d\bar{\phi}(\boldsymbol{x}, t)}{dt} = \overline{\frac{d\phi}{dt}}(\boldsymbol{x}, t) + \beta_t(\phi), \tag{A29}$$

where $\beta_t(\phi)$ is defined as

$$\beta_t(\phi) = \int_{\mathbb{R}^3} \hat{\phi}(\boldsymbol{\kappa}, t) \frac{d\hat{G}_{\kappa_c}(\boldsymbol{\kappa}, t)}{dt} e^{i\boldsymbol{\kappa x}} d\boldsymbol{\kappa}. \tag{A30}$$

For a box filter in the spectral size,

$$\hat{G}_{\kappa_c}(\boldsymbol{\kappa}, t) = H(\boldsymbol{\kappa_c} - \boldsymbol{\kappa}, t), \tag{A31}$$

where H denotes the Heaviside distribution verifying

$$\frac{dH(\boldsymbol{\kappa_c} - \boldsymbol{\kappa}, t)}{dt} = \frac{d\boldsymbol{\kappa_c}}{dt} \delta(\boldsymbol{\kappa_c} - \boldsymbol{\kappa}, t), \tag{A32}$$

and where δ is the Dirac distribution. Using Eq. (A32), Eq. (A30) becomes

$$\beta_t(\phi) = \frac{d\boldsymbol{\kappa_c}}{dt} \int_{\mathbb{R}^3} \hat{\phi}(\boldsymbol{\kappa}, t) \delta(\boldsymbol{\kappa_c} - \boldsymbol{\kappa}, t) e^{i\boldsymbol{\kappa x}} d\boldsymbol{\kappa}. \tag{A33}$$

Introducing the spherical coordinates, $\kappa_1 = \kappa \sin\theta \cos\phi$, $\kappa_2 = \kappa \sin\theta \sin\phi$, and $\kappa_3 = \kappa \cos\theta$, one finds finally

$$\beta_t(\phi) = \frac{d\kappa_c}{dt} \oiint_{\kappa^2 = \kappa_c^2} \hat{\phi}(\boldsymbol{\kappa}, t) e^{i\boldsymbol{\kappa x}} dA(\kappa). \tag{A34}$$

4. Energy density spectrum variation through the cutoff wave number

We consider homogeneous turbulent flows. The transport equation for the filtered turbulence energy (43) can be written using as well κ_c as the filter size parameter, the equation readily transforms into

$$\frac{D}{Dt}\left(\frac{\overline{u}_i\overline{u}_i}{2}\right) = \overline{u}_i\overline{\frac{du_i}{dt}} + \frac{\partial \kappa_c}{\partial t}\frac{\partial}{\partial \kappa_c}\left(\frac{\overline{u}_i\overline{u}_i}{2}\right) + \overline{u}_j\frac{\partial \kappa_c}{\partial x_j}\frac{\partial}{\partial \kappa_c}\left(\frac{\overline{u}_i\overline{u}_i}{2}\right) - \overline{u}_i\frac{\partial \tau(u_j,u_i)}{\partial x_j} + \overline{u}_j\frac{\partial \kappa_c}{\partial x_j}\frac{\partial \tau(u_j,u_i)}{\partial \kappa_c}. \tag{A35}$$

The corresponding statistical equation in the particular case of strictly homogeneous turbulence with a time evolution of the filter size is then given by Eq. (62)

$$\frac{\partial}{\partial t}\left\langle\frac{\bar{u}_i\bar{u}_i}{2}\right\rangle = \left\langle\bar{u}_i\overline{\frac{du_i}{dt}}\right\rangle + \frac{\partial \kappa_c}{\partial t}\frac{\partial}{\partial \kappa_c}\left\langle\frac{\bar{u}_i\bar{u}_i}{2}\right\rangle - \left\langle\bar{u}_i\frac{\partial \tau_{ij}}{\partial x_j}\right\rangle. \tag{A36}$$

The resolved stresses are defined as in Ref. 36

$$(\tau_{ij})_r = \bar{u}_i\bar{u}_j - \langle u_i\rangle\langle u_j\rangle \tag{A37}$$

and for the resolved turbulence kinetic energy, the result is obtained by tensorial contraction

$$k_r = \frac{1}{2}\left[\bar{u}_j\bar{u}_j - \langle u_j\rangle\langle u_j\rangle\right]. \tag{A38}$$

The statistical turbulent energy is then derived by taking the mean value of Eq. (A38) in the statistical sense leading to

$$\langle k_r\rangle = \frac{1}{2}[\langle\bar{u}_i\bar{u}_i\rangle - \langle u_i\rangle\langle u_i\rangle]. \tag{A39}$$

It is straightforward to relate the resolved turbulence kinetic energy given by Eq. (A39) to the density spectrum:

$$\langle k_r\rangle = \frac{1}{2}[\langle\bar{u}_i\bar{u}_i\rangle - \langle u_i\rangle\langle u_i\rangle] = \frac{1}{2}\left\langle u_i^{<}u_i^{<}\right\rangle = \int_0^{\kappa_C} E(\kappa)d\kappa, \tag{A40}$$

with $u_i^{<} = \bar{u}_i - \langle u_i\rangle$. Remarking that the statistical mean velocity $\langle u_i\rangle$ does not depend on the cutoff wave number κ_c while the mean energy $\langle\overline{u}_i\overline{u}_i\rangle/2$ does depend on κ_c, the derivative of Eq. (A40) then yields

$$\frac{\partial\langle k_r\rangle}{\partial \kappa_c} = \frac{\partial}{\partial \kappa_c}\left\langle\frac{\bar{u}_i\bar{u}_i}{2}\right\rangle = E(\kappa_c, t). \tag{A41}$$

So that Eq. (A36) becomes

$$\frac{\partial}{\partial t}\left\langle\frac{\bar{u}_i\bar{u}_i}{2}\right\rangle = \left\langle\bar{u}_i\overline{\frac{du_i}{dt}}\right\rangle + E(\kappa_c, t)\frac{\partial \kappa_c}{\partial t} - \left\langle\bar{u}_i\frac{\partial \tau_{ij}}{\partial x_j}\right\rangle. \tag{A42}$$

It can easily be shown that similar relations hold for the double velocity correlations, their derivation is straightforward

$$\frac{\partial}{\partial t}\left\langle\frac{1}{2}\bar{u}_i\bar{u}_j\right\rangle = \left\langle\bar{u}_i\overline{\frac{du_j}{dt}}\right\rangle + \left\langle\bar{u}_j\overline{\frac{du_i}{dt}}\right\rangle + \varphi_{ij}(\kappa_c, t)\frac{\partial \kappa_c}{\partial t} - \left\langle\bar{u}_j\frac{\partial \tau_{ik}}{\partial x_k}\right\rangle - \left\langle\bar{u}_i\frac{\partial \tau_{jk}}{\partial x_k}\right\rangle, \tag{A43}$$

where φ_{ij} is the three-dimensional spectral tensor of the double velocity correlations, such that $\varphi_{jj}/2 = E$. These extra terms coming from the material derivative are thus interpreted as spectral fluxes. In this form, they were an essential feature of the split spectrum statistical approach introduced in Refs. 20–22. Equation (A42) can be rewritten using the partial derivative in time of Eq. (A40). As a result, one then obtains

$$\frac{\partial}{\partial t}\int_0^{\kappa_c} E(\kappa, t)d\kappa = \left\langle\bar{u}_i\overline{\frac{du_i}{dt}}\right\rangle - \frac{\partial}{\partial t}\left(\frac{\langle u_i\rangle\langle u_i\rangle}{2}\right) - \left\langle\bar{u}_i\frac{\partial \tau_{ij}}{\partial x_i}\right\rangle + E(\kappa_c, t)\frac{\partial \kappa_c}{\partial t}. \tag{A44}$$

On the other hand, the partial derivative in time of the three-dimensional turbulence kinetic energy spectrum $E(\kappa, t)$ is given by

$$\frac{\partial}{\partial t}\int_0^{\kappa_c} E(\kappa, t)d\kappa = \int_0^{\kappa_c} \frac{\partial E(\kappa, t)}{\partial t}d\kappa + E(\kappa_c)\frac{\partial \kappa_c}{\partial t}. \tag{A45}$$

The correspondence with Eq. (A44) is then straightforward.

5. Improved approximation proposal

As we have seen, the commutation term in the material derivative of the turbulence kinetic energy is

$$\frac{1}{2}\beta_T(u_i u_i) - \bar{u}_i \beta_T(u_i) = \frac{D\kappa_c}{Dt}\frac{\partial k_{sfs}}{\partial \kappa_c} \tag{A46}$$

using κ_c instead of Δ. This equation can be easily related to the energy spectrum by remarking that

$$\frac{\partial \langle k_{sfs}\rangle}{\partial \kappa_c} = \frac{\partial}{\partial \kappa_c}\int_{\kappa_c}^{\infty} E(\kappa)d\kappa = -E(\kappa_c). \tag{A47}$$

Assuming that the spectrum follows a Kolmogorov law in (−5/3) such as $E(\kappa) = C_\kappa \epsilon^{2/3}\kappa^{-5/3}$ (more generally any m power law could be experimented), it is possible to compute $\langle \widetilde{k_{sfs}}\rangle - \langle k_{sfs}\rangle$ as

$$\langle \widetilde{k_{sfs}}\rangle - \langle k_{sfs}\rangle = \int_{\widetilde{\kappa}_c}^{\kappa_c} C_\kappa \epsilon^{2/3}\kappa^{-5/3}d\kappa = -\frac{3}{2}C_\kappa \epsilon^{2/3}\left[\frac{1}{\kappa_c^{2/3}} - \frac{1}{\widetilde{\kappa}_c^{2/3}}\right]. \tag{A48}$$

This equation allows to compute $C_\kappa \epsilon^{2/3}$ that is then introduced in the expression of the spectrum $E(\kappa_c)$ leading to

$$E(\kappa_c) = -\frac{2}{3}(\langle \widetilde{k_{sfs}}\rangle - \langle k_{sfs}\rangle)\frac{\widetilde{\kappa}_c^{2/3}}{(\widetilde{\kappa}_c^{2/3} - \kappa_c^{2/3})\kappa_c}, \tag{A49}$$

with $\langle \widetilde{k_{sfs}}\rangle > \langle k_{sfs}\rangle$ and $\widetilde{\kappa}_c < \kappa_c$. So that Eq. (A46) becomes in the mean

$$\frac{D\kappa_c}{Dt}\frac{\partial \langle k_{sfs}\rangle}{\partial \kappa_c} = -E(\kappa_c)\frac{D\kappa_c}{Dt} = \frac{2}{3}\frac{D\kappa_c}{Dt}\left(\frac{\widetilde{\kappa}_c^{2/3}}{\kappa_c}\right)\left(\frac{\langle \widetilde{k_{sfs}}\rangle - \langle k_{sfs}\rangle}{\widetilde{\kappa}_c^{2/3} - \kappa_c^{2/3}}\right). \tag{A50}$$

Supposing now that the relation also holds approximately for the instantaneous quantities, we get

$$\frac{1}{2}\beta_T(u_i u_i) - \bar{u}_i \beta_T(u_i) = \frac{2}{3}\frac{D\kappa_c}{Dt}\left(\frac{\widetilde{\kappa}_c^{2/3}}{\kappa_c}\right)\left(\frac{\widetilde{k_{sfs}} - k_{sfs}}{\widetilde{\kappa}_c^{2/3} - \kappa_c^{2/3}}\right). \tag{A51}$$

Comparing to the standard approximation

$$\frac{1}{2}\beta_T(u_i u_i) - \overline{u}_i \beta_T(u_i) \approx \frac{D\kappa_c}{Dt}\left(\frac{\widetilde{k_{sfs}} - k_{sfs}}{\widetilde{\kappa}_c - \kappa_c}\right), \tag{A52}$$

one would be led to

$$\frac{1}{2}\beta_T(u_i u_i) - \overline{u}_i \beta_T(u_i) \approx f_{corr}\frac{D\kappa_c}{Dt}\left(\frac{\widetilde{k_{sfs}} - k_{sfs}}{\widetilde{\kappa}_c - \kappa_c}\right), \tag{A53}$$

with a possible correction factor to use in practical simulations

$$f_{corr} = \frac{2}{3}\left(\frac{\widetilde{\kappa}_c^{2/3}}{\kappa_c^{2/3} - \widetilde{\kappa}_c^{2/3}}\right)\left(\frac{\kappa_c - \widetilde{\kappa}_c}{\kappa_c}\right). \tag{A54}$$

[1] M. Lesieur and O. Metais, "New trends in large-eddy simulations of turbulence," Ann. Rev. J. Fluid Mech. **28**, 45 (1996).
[2] P. R. Spalart, "Detached-eddy simulation," Annu. Rev. Fluid Mech. **41**, 181 (2009).
[3] B. Chaouat, "Reynolds stress transport modeling for high-lift airfoil flows," AIAA J. **44**, 2390 (2006).
[4] T. B. Gatski, C. L. Rumsey, and R. Manceau, "Current trends in modelling research for turbulent aerodynamic flows," Philos. Trans. R. Soc. London, Ser. A **365**, 2389 (2007).

[5] J. Fröhlich and D. Von Terzi, "Hybrid LES/RANS methods for the simulation of turbulent flows," Prog. Aerosp. Sci. **44**, 349 (2008).
[6] R. Schiestel and A. Dejoan, "Towards a new partially integrated transport model for coarse grid and unsteady turbulent flow simulations," Theor. Comput. Fluid Dyn. **18**, 443 (2005).
[7] B. Chaouat and R. Schiestel, "A new partially integrated transport model for subgrid-scale stresses and dissipation rate for turbulent developing flows," Phys. Fluids **17**, 065106 (2005).
[8] L. C. Berselli, T. Iliescu, and W. J. Layton, *Mathematics of Large Eddy Simulation of Turbulent Flows* (Springer, Berlin, 2006), pp. 227–251.
[9] S. Ghosal and P. Moin, "The basic equations for large eddy simulation of turbulent flows in complex geometries," J. Comput. Phys. **118**, 24 (1995).
[10] H. Van der Ven, "A family of large eddy simulation (LES) filters with nonuniform filter widths," Phys. Fluids **7**, 1171 (1995).
[11] C. Fureby and G. Tabor, "Mathematical and physical constraints on large-eddy simulations," Theor. Comput. Fluid Dyn. **9**, 85 (1997).
[12] O. V. Vasilyev, T. S. Lund, and P. Moin, "A general class of commutative filters for LES in complex geometries," J. Comput. Phys. **146**, 82 (1998).
[13] A. L. Marsden, O. V. Vasilyev, and P. Moin, "Construction of commutative filters for LES on unstructured meshes," J. Comput. Phys. **175**, 584 (2002).
[14] M. Iovieno and D. Tordella, "Variable scale filtered Navier-Stokes equations: A new procedure to deal with the associated commutation error," Phys. Fluids **15**, 1926 (2003).
[15] O. V. Vasilyev and D. E. Goldstein, "Local spectrum of commutation error in large eddy simulations," Phys. Fluids **16**, 470 (2004).
[16] F. Hamba, "Analysis of filtered Navier-Stokes equation for hybrid RANS/LES simulation," Phys. Fluids **23**, 015108 (2011).
[17] F. Hamba, "A hybrid RANS/LES simulation of turbulent channel flow," Theor. Comput. Fluid Dyn. **16**, 387 (2003).
[18] U. Piomelli, E. Balaras, H. Pasinato, K. D. Squires, and P. R. Spalart, "The inner-outer layer interface in large-eddy simulations with wall-layer models," Int. J. Heat Fluid Flow **24**, 538 (2003).
[19] F. Hamba, "A hybrid RANS/LES simulation of high-Reynolds-number channel flow using additional filtering at the interface," Theor. Comput. Fluid Dyn. **20**, 89 (2006).
[20] R. Schiestel, "Sur le concept d'échelles multiples en modélisation des écoulements turbulents, Part I," J. Theor. Appl. Mech. **2**(3), 417 (1983).
[21] R. Schiestel, "Sur le concept d'échelles multiples en modélisation des écoulements turbulents, Part II," J. Theor. Appl. Mech. **2**(4), 601 (1983).
[22] R. Schiestel, "Multiple-time scale modeling of turbulent flows in one point closures," Phys. Fluids **30**, 722 (1987).
[23] A. Cubero and U. Piomelli, "Large eddy simulations of channel flows with variable filter-width-to-grid-size ratios," in *Direct and Large Eddy Simulation VI*, ERCOFTAC Vol. 10, edited by E. Lamballais, R. Friedrich, B. J. Geurts, and O. Métais (Kluwer Academic, 2006), pp. 151–158.
[24] J. Fröhlich, J. A. Denev, C. Hinterberger, and H. Bockhorn, "On the impact of tangential grid refinement on subgrid scale modelling in large eddy simulation," in *6th International Conference on Numerical Method and Applications (NMA), 2006*, edited by T. Boyanov, S. Dimova, K. Georgiev, and G. Nikolov (Springer, 2007), pp 550–557.
[25] F. van des Bos and B. J. Geurts, "Dynamic of commutator-errors in LES with non-uniform filter width," in *Direct and Large Eddy Simulation V*, ERCOFTAC Vol. 9, edited by R. Friedrich, B. J. Geurts, and O. Métais (Kluwer Academic, 2004), pp. 155–162.
[26] F. van der Bos and B. J. Geurts, "Commutator errors in the filtering approach to large-eddy simulation," Phys. Fluids **17**, 035108 (2005).
[27] F. van der Bos and B. J. Geurts, "Lagrangian dynamics of commutator errors in large eddy simulation," Phys. Fluids **17**, 075101 (2005).
[28] B. J. Geurts and D. H. Holm, "Commutator errors in large eddy simulation," J. Phys. A **39**, 2213 (2006).
[29] S. S. Girimaji and S. Wallin, "Closures modeling in bridging regions of variable-resolution (VR) turbulence computations," J. Turbul. **14**, 72 (2013).
[30] C. D. Pruett, "Eulerian time-domain filtering for spatial large-eddy simulation," AIAA J. **38**, 1634 (2000).
[31] C. D. Pruett, T. B. Gatski, C. E. Grosch, and W. D. Thacker, "The temporally filtered Navier-Stokes equations: Properties of the residual stress," Phys. Fluids **15**, 2127 (2003).
[32] D. Jeandel, J. F. Brison, and J. Mathieu, "Modeling methods in physical and spectral space," Phys. Fluids **21**, 169 (1978).
[33] C. Cambon, D. Jeandel, and J. Mathieu, "Spectral modelling of homogeneous non-isotropic turbulence," J. Fluid Mech. **104**, 247 (1981).
[34] W. J. T. Bos and J. P. Bertoglio, "Inertial range scaling of scalar flux spectra in uniformly sheared turbulence," Phys. Fluids **19**, 025104 (2007).
[35] H. Touil, J. P. Bertoglio, and S. Parpais, "A spectral closure applied to anisotropic inhomogeneous turbulence," in *Proceedings of the Eighth European Turbulence Conference*, Advances in Turbulence Vol. VIII, edited by C. Dopazo (CIMNE, Barcelona, 2010), pp. 689–692.
[36] B. Chaouat and R. Schiestel, "From single-scale turbulence models to multiple-scale and subgrid-scale models by Fourier transform," Theor. Comput. Fluid Dyn. **21**, 201 (2007).
[37] R. Schiestel, *Modeling and Simulation of Turbulent Flows* (ISTE Ltd, 2008).
[38] M. Germano, "Turbulence: The filtering approach," J. Fluid Mech. **238**, 325 (1992).
[39] M. Germano, "The simplest decomposition of a turbulent field," Physica D **241**, 284 (2012).
[40] B. Chaouat, "Simulation of turbulent rotating flows using a subfilter scale stress model derived from the partially integrated transport modeling method," Phys. Fluids **24**, 045108 (2012).

[41] B. Chaouat and R. Schiestel, "Analytical insights into the partially integrated transport modeling method for hybrid Reynolds averaged Navier-Stokes equations-large eddy simulations of turbulent flows," Phys. Fluids **24**, 085106 (2012).
[42] A. Scotti, C. Meneveau, and D. K. Lilly, "Generalized Smagorinsky model for anisotropic grids," Phys. Fluids **5**, 2306 (1993).
[43] B. Chaouat and R. Schiestel, "Progress in subgrid-scale transport modelling for continuous hybrid non-zonal RANS/LES simulations," Int. J. Heat Fluid Flow **30**, 602 (2009).
[44] S. C. Crow, "Viscoelastic properties of the fine-grained incompressible turbulence," J. Fluid Mech. **33**, 1 (1968).
[45] B. Chaouat, "Subfilter-scale transport model for hybrid RANS/LES simulations applied to a complex bounded flow," J. Turbul. **11**, 51 (2010).
[46] B. Chaouat and R. Schiestel, "Hybrid RANS-LES simulations of the turbulent flow over periodic hills at high Reynolds number using the PITM method," Comput. Fluids **84**, 279 (2013).
[47] B. Chaouat, "Numerical predictions of channel flows with fluid injection using Reynolds stress model," J. Propul. Power **18**, 295 (2002).
[48] B. Chaouat, "An efficient numerical method for RANS/LES turbulent simulations using subfilter scale stress transport equations," Int. J. Numer. Methods Fluids **67**, 1207 (2011).
[49] Ph. Roy, "Résolution des équations de Navier-Stokes par un schéma de haute précision en espace et en temps," Rech. Aerosp. **6**, 373 (1980).
[50] R. S. Rogallo, "An ILLIAC program for the numerical simulation of homogeneous incompressible turbulence," NASA Tech. Memo 73203, edited by NASA Ames Research Center, California, 1977.
[51] M. J. Lee and W. C. Reynolds, "Numerical experiments on the structure of homogeneous turbulence," NASA Tech. Memo NCC-2-15, Report No. TF-24, edited by Stanford University, California, 1985.
[52] J. H. Ferziger and M. Peric, *Computational Methods for Fluid Dynamics*, 3rd ed. (Springer, New York, 2002).
[53] C. Hertel, M. Schümichen, J. Lang, and J. Fröhlich, "Using a moving mesh PDE for cell centres to adapt a finite volume grid," Flow Turbul. Combust. **90**, 785 (2013).